

W K McGregor



**SPECTRAL SIMULATION OF RESONANCE BAND
TRANSMISSION PROFILES FOR SPECIES
CONCENTRATION MEASUREMENTS:
NO γ -BANDS AS AN EXAMPLE**

M. G. Davis, W. K. McGregor, and J. D. Few
ARO, Inc.

**ENGINE TEST FACILITY
ARNOLD ENGINEERING DEVELOPMENT CENTER
AIR FORCE SYSTEMS COMMAND
ARNOLD AIR FORCE STATION, TENNESSEE 37389**

January 1975

Interim Report for Period FY 73 and FY 74

Approved for public release; distribution unlimited.

Prepared for

**DIRECTORATE OF TECHNOLOGY
ARNOLD ENGINEERING DEVELOPMENT CENTER
ARNOLD AIR FORCE STATION, TENNESSEE 37389**



DOC NUM SER CN
UNC29812-PDC A 1

NOTICES

When U. S. Government drawings specifications, or other data are used for any purpose other than a definitely related Government procurement operation, the Government thereby incurs no responsibility nor any obligation whatsoever, and the fact that the Government may have formulated, furnished, or in any way supplied the said drawings, specifications, or other data, is not to be regarded by implication or otherwise, or in any manner licensing the holder or any other person or corporation, or conveying any rights or permission to manufacture, use, or sell any patented invention that may in any way be related thereto.

Qualified users may obtain copies of this report from the Defense Documentation Center.

References to named commercial products in this report are not to be considered in any sense as an endorsement of the product by the United States Air Force or the Government.

This report has been reviewed by the Information Office (OI) and is releasable to the National Technical Information Service (NTIS). At NTIS, it will be available to the general public, including foreign nations.

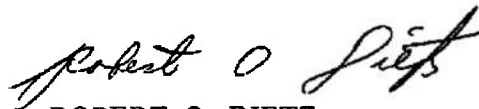
APPROVAL STATEMENT

This technical report has been reviewed and is approved for publication.

FOR THE COMMANDER



EULES L. HIVELY
Research and Development
Division
Directorate of Technology



ROBERT O. DIETZ
Director of Technology

UNCLASSIFIED

REPORT DOCUMENTATION PAGE		READ INSTRUCTIONS BEFORE COMPLETING FORM
1 REPORT NUMBER AEDC-TR-74-124	2 GOVT ACCESSION NO.	3 RECIPIENT'S CATALOG NUMBER
4. TITLE (and Subtitle) SPECTRAL SIMULATION OF RESONANCE BAND TRANSMISSION PROFILES FOR SPECIES CONCENTRATION MEASUREMENTS: NO γ-BANDS AS AN EXAMPLE		5. TYPE OF REPORT & PERIOD COVERED Interim Report-FY 73 and FY 74
7. AUTHOR(s) M. G. Davis, W. K. McGregor, and J. D. Few, ARO, Inc.		6. PERFORMING ORG REPORT NUMBER
9 PERFORMING ORGANIZATION NAME AND ADDRESS Arnold Engineering Development Center Arnold Air Force Station, Tennessee 37389		8 CONTRACT OR GRANT NUMBER(s)
11 CONTROLLING OFFICE NAME AND ADDRESS Arnold Engineering Development Center (DYFS), Arnold Air Force Station, Tennessee 37389		10. PROGRAM ELEMENT, PROJECT, TASK AREA & WORK UNIT NUMBERS Program Element 65802F
14 MONITORING AGENCY NAME & ADDRESS (if different from Controlling Office)		12. REPORT DATE January 1975
15. SECURITY CLASS. (of this report) UNCLASSIFIED		13 NUMBER OF PAGES 51
16 DISTRIBUTION STATEMENT (of this Report) Approved for public release; distribution unlimited.		15a. DECLASSIFICATION/DOWNGRADING SCHEDULE N/A
17 DISTRIBUTION STATEMENT (of the abstract entered in Block 20, if different from Report)		
18 SUPPLEMENTARY NOTES Available in DDC		
19 KEY WORDS (Continue on reverse side if necessary and identify by block number) spectra transmitting simulation profiles resonance measurements (concentration) band spectra		
20 ABSTRACT (Continue on reverse side if necessary and identify by block number) The equations necessary for the calculation of the integrated transmission of overlapped, Doppler-Broadened spectral lines through a medium at a specified density, temperature, and path length are developed in conjunction with a computation procedure for simulation of a spectrometer output. The application is then made to resonance absorption by diatomic molecules. Existing band transmission data for the (0,0) band of the γ-system of the		

UNCLASSIFIED

UNCLASSIFIED

20. ABSTRACT (Continued)

nitric oxide molecule at low pressures are used to test the calculations. Satisfactory agreement between measured and calculated transmission spectral profiles was obtained.

PREFACE

The research reported herein was carried out under sponsorship of the USAF Arnold Engineering Development Center (AEDC) under Program Element 65802F. The results of this research program were obtained by ARO, Inc. (a subsidiary of Sverdrup & Parcel and Associates, Inc.), contract operator of AEDC, Air Force Systems Command (AFSC), Arnold Air Force Station, Tennessee. The work was accomplished in the Engine Test Facility (ETF), under ARO Project Numbers RF405 and RF425. The manuscript (ARO Control No. ARO-ETF-TR-74-73) was submitted for publication on August 21, 1974.

The authors extend special acknowledgment to Mr. Howard Glassman (Central Computer Operations, ARO, Inc) who wrote the computer code for simulation of the spectral radiation.

Dr. M. G. Davis is an Associate Professor of Physics at the University of Tennessee at Nashville and consultant to ARO, Inc.

CONTENTS

	<u>Page</u>
1.0 INTRODUCTION	7
2.0 THEORETICAL DEVELOPMENT	
2.1 Development of Transmission Formulae for Overlapping Lines	10
2.2 Relation Between Absorption Coefficient and Absorbing Medium Properties	12
2.3 Simulation of Spectral Bands	14
3.0 APPLICATION OF THE BAND ABSORPTION TECHNIQUE TO THE NITRIC OXIDE (NO) MOLECULE	
3.1 Description of Experimental Data	15
3.2 Source Characteristics	17
3.3 Simulated Spectral Calculations	20
3.4 Comparisons and Applications	26
4.0 DISCUSSION	
4.1 Problem Areas and Limitations	28
4.2 Utility of the Method	35
5.0 SUMMARY OF RESULTS	36
REFERENCES	36

ILLUSTRATIONS

Figure

1. Illustration of Overlapping Absorption Lines	9
2. Illustration of Physical Arrangement for Spectral Line Absorption Measurements	15
3. (0,0) Band of the NO γ -System Obtained from Discharge Tube Containing a Mixture of 12:3:1 (by volume) of A:N ₂ :O ₂ at 8 Torr with 2800 Volts Applied by Use of 1-Meter Spectrometer in Second Order (Equivalent Slit Width, 0.03Å)	16
4. (0,0) Band of the NO γ -System Obtained from Discharge Tube Containing a Mixture of 12:3:1 (by volume) of A:N ₂ :O ₂ at 8 Torr with 2800 Volts Applied by Use of 1/2-Meter Spectrometer in First Order (Equivalent Slit Width, 1.6Å)	17
5. Measured Spectral (Bandpass - 1.6Å) Profile for Transmission of the (0,0) Band of the NO γ - System through 300°K NO at Selected Values of Gas Pressure and a Fixed Path Length (44.1 cm) from a Gas Discharge Tube Containing a 12:3:1 Mixture (by volume) of A:N ₂ :O ₂ and Operating at 8 Torr with 2800 Volts Applied and Estimated Temperature of 320°K	18

<u>Figure</u>	<u>Page</u>
6. Diagram of Resonance Lamp Used to Produce Narrow-Line Radiation	19
7. Population Distribution of Excited Rotational States of the $A^2\Sigma$ Level of NO in a Water-Cooled Discharge Tube Operated at 8 Torr with 2800 Volts Applied and Containing a 12:3:1 Mixture (by volume) of A:N ₂ :O ₂	20
8. Illustrative Spectral Simulation Plot for the (0,0) Band of NO	22
9. Calculated Spectral Plots of the NO (0,0) γ -Band Corresponding to Transmission of Radiation from a Discharge Lamp Source Containing a 12:3:1 Mixture (by volume) of A:N ₂ :O ₂ and Operated at 8 Torr with 2800 Volts Applied, through Media Having Several Values of the Optical Path Length ($N_0\ell$)	23
10. Comparison of Measured and Calculated Transmissivity through Pure NO at 300°K as a Function of the Optical Path Length ($N_0\ell$) for the $Q_{22}(23/2) + R_{12}(23/2)$ Line of the (0,0) Band of the NO γ -System from a 320°K Source	26
11. Calculated Spectral (Bandpass - 1.6Å) Profile for Transmission of the (0,0) Band of the NO γ -System through 300°K NO at Selected Values of Gas Pressure, a Fixed Path Length (44.1 cm), and for a 320°K Source with Line Distribution Corresponding to Discharge Tube Pressure of 8 Torr and 2800 Volts Applied	27
12. Comparison of Measured and Computed Calibration Curves for Transmissivity at the Wavelength of the Second Bandhead of the (0,0) Band of the NO γ -System versus $N_0\ell$ for 300°K Absorbing Gas, 320°K Source Gas and for a Source Line Distribution Corresponding to Discharge Tube Pressure of 8 Torr and 2800 Volts Applied	29
13. Comparison of Measured and Computed Calibration Curves for Transmissivity Integrated over Entire (0,0) Band of the NO γ -System versus $N_0\ell$ for 300°K Absorbing Gas, 320°K Source Gas, and for a Source Line Distribution Corresponding to Discharge Tube Pressure of 8 Torr and 2800 Volts Applied	30

<u>Figure</u>	<u>Page</u>
14. Computed Calibration Curves for Transmissivity at the Wavelength of the Second Bandhead of the (0,0) Band of the NO γ -System versus $N_0\ell$ with Absorber Temperature (T_a) as a Parameter for 320°K Source Temperature and a Source Line Distribution Corresponding to Discharge Tube Pressure of 8 Torr and 2800 Volts Applied	31
15. Computed Calibration Curves for Transmissivity Integrated over Entire (0,0) Band of the NO γ -System versus $N_0\ell$ with Absorber Temperature (T_a) as a Parameter for 320°K Source Temperature and a Source Line Distribution Corresponding to Discharge Tube Pressure of 8 Torr and 2800 Volts Applied	32

APPENDIX

A. METHOD OF SIMULATION OF SPECTRAL BAND PROFILES FROM REAL INSTRUMENTS	39
NOMENCLATURE	49

1.0 INTRODUCTION

In many areas of testing of aerospace and aerodynamic vehicles at the Arnold Engineering Development Center (AEDC), the requirement is imposed to measure individual molecular species densities. Several different techniques are used to accomplish such measurements. The most common technique is to insert a sampling probe into a gas stream and extract and analyze a sample using conventional process instruments. The major disadvantages of this procedure are the disturbance effects of the probe on the gas stream and the change in species due to chemical reactions within the sampling transfer lines. A more desirable procedure is to use a method which does not disturb the gas stream and thus measures the species concentration in situ. For a great many applications, absorption spectroscopy fulfills the requirements for an in situ measurement.

The use of absorption spectroscopy for density measurements may take on many forms depending upon the application and the molecule involved. The most common method employs a continuum source in the infrared. However, in combustion gases the infrared spectrum is overlapped by bands of different molecules; isolation of species other than the major components, water vapor and carbon dioxide, is difficult. Another method which has found utility in many instances is the spectral line absorption method in which a line source in the visible or ultraviolet spectral region is employed which has the same wavelength as the resonance lines or bands of the absorbing species. The absorption method is useful for atoms and also for molecules which have a resonance transition. Several diatomic, heteronuclear molecules which occur in combustion exhaust products have resonance transitions in spectral regions which are accessible with conventional spectrometric apparatus. The governing equations for the line absorption method are developed in the classical text by Mitchell and Zemansky (Ref. 1), and some applications are described in Refs. 2, 3, and 4.

A particularly effective method of conducting the line absorption measurement is to use a source in which the lines have a much narrower width than the absorption lines. In this case the measured absorption coefficient is the line center absorption coefficient which is simply and directly related to the species concentration. Unfortunately, the narrow line situation is encountered only occasionally; in the more usual application a difficult integral over the source line and absorption line shapes must be performed (Ref. 1).

A difficulty which is encountered in the practical realm of measurement of molecular concentrations using the line ab-

sorption method is that the lines within a band cannot be isolated due to overlapping of the lines or limitations of the spectrometric equipment which must be employed for field measurements. This lack of isolation makes the interpretation of absorption measurements from first principles a difficult task, and investigators have usually gone to laboratory calibrations in such cases. However, the calibration route becomes very tedious because of the dependence of the absorption on temperature, and the method is seriously impaired when there are temperature gradients along the optical path. The equations which must be solved in order to determine species densities and temperature directly from absorption measurements are developed in this report.

The resonance absorption technique has been applied at AEDC to measure the OH and NO molecular densities in the exhaust of a turbojet engine being operated at simulated high altitude conditions (Ref. 4). For OH, several lines in the 3064 Å resonance band were spaced sufficiently far apart that lines could be isolated by the 1/2-meter spectrometer which was used and the line absorption method could be used in its most simple form. For NO, the lines of the resonance γ -bands are more closely spaced than those of OH and could not be resolved using the 1/2-meter spectrometer. Therefore, a laboratory calibration had to be used. The calibration was performed using pure NO in a low pressure, room temperature absorption cell. The approach used was to correct the measured transmission to line center transmission, assuming that Doppler broadening was prevalent over other broadening mechanisms. The results of the measurements were that the NO concentration measured by the absorption technique was much larger than that measured by sampling techniques. Because of this discrepancy and because the calibration at room temperature was recognized as a weak link in the absorption technique, an analytical investigation was initiated to develop computational procedures for predicting the transmission of resonance radiation through media under any conditions of temperature and pressure.

This report presents the development of a general procedure for analytically determining, from first principles, the spectral band absorption as a function of temperature and concentration. The procedure is applied to the (0,0) band of the NO γ -system for temperatures ranging from 300°K to 2000°K and for densities ranging from 10^{15} molecules/cm³ to 10^{18} molecules/cm³. In this application, the absorbing gas is pure NO and, thus, the total pressure is very low. At low pressures, Doppler broadening is the predominant broadening mechanism, and for this report Lorentz and natural broadening are considered negligible. The calculated band profiles in transmission will

be compared to experimental data in a number of ways in this report.

2.0 THEORETICAL DEVELOPMENT

Two problems are encountered in the determination of species densities from band absorption measurements. The first problem arises because of the overlapping of lines due to their finite width and close spacing. The second problem arises because of the inability of spectrometers to resolve individual spectral lines, which affects the interpretation of transmission measurements. The first difficulty lies in the fact that the transmission of a particular emission line from a source is affected by both its corresponding absorption line and those absorption lines in close proximity, as illustrated in Fig. 1. The correct treatment of the problem requires that, for each emission line, the absorption of all lines in close proximity be accounted for.

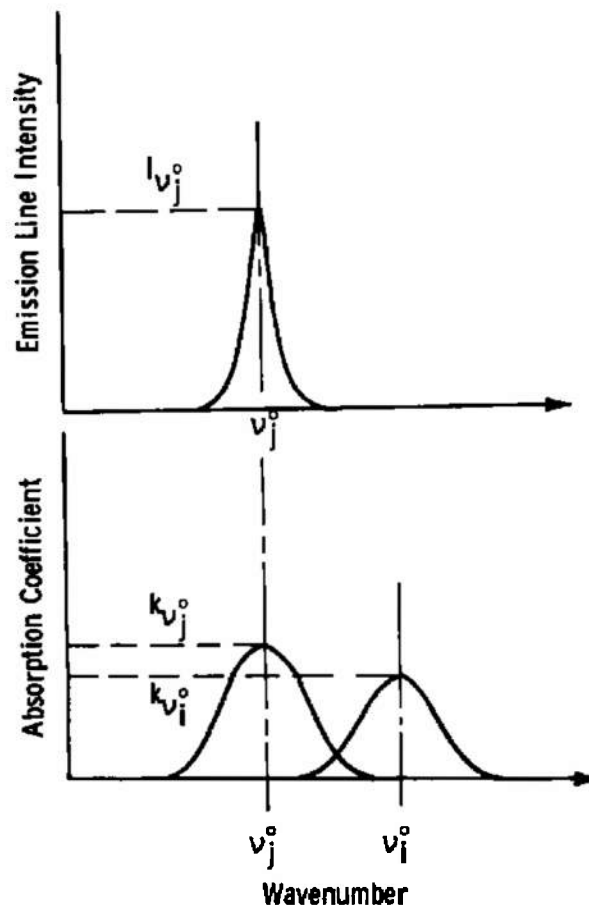


Figure 1. Illustration of overlapping absorption lines.

2.1 DEVELOPMENT OF TRANSMISSION FORMULAE FOR OVERLAPPING LINES

For a single, isolated j^{th} spectral line, the transmission, \bar{T}_j , of a source line having some frequency distribution, $I_{\nu_j}^0$, through a uniform absorbing medium of length ℓ is given by

$$\bar{T}_j = \int_0^{\infty} I_{\nu_j}^0 \exp(-k_{\nu_j} \ell) d\nu_j \quad (1)$$

where k_{ν_j} is the absorption coefficient which has a frequency distribution independent of $I_{\nu_j}^0$. In many cases both $I_{\nu_j}^0$ and k_{ν_j} may simply be given by the Doppler broadening expression,

$$I_{\nu_j}^0 = I_{\nu_j^0}^0 \exp \left\{ - \left[\frac{2(\nu - \nu_j^0)}{(\Delta_S \nu_j)_D} \sqrt{\ln 2} \right]^2 \right\} \quad (2)$$

$$k_{\nu_j} = k_{\nu_j^0} \exp \left\{ - \left[\frac{2(\nu - \nu_j^0)}{(\Delta_a \nu_j)_D} \sqrt{\ln 2} \right]^2 \right\} \quad (3)$$

where $I_{\nu_j^0}^0$ is the intensity of the source line at center frequency, ν_j^0 , and $(\Delta_S \nu_j)_D$ is the Doppler width at half the intensity (half-width) at line center of the emitted spectral line, given by

$$(\Delta_S \nu_j)_D = 2 \nu_j^0 \sqrt{\frac{2 \ln 2 \kappa T_s}{M_s c^2}} \quad (4)$$

In Eq. (4), κ is Boltzmann's constant, T_s is the absolute temperature of the source, and M_s is the mass of the emitting molecule. The Doppler half width of the absorbing line is given by

$$(\Delta_a \nu_j)_D = 2 \nu_j^0 \sqrt{\frac{2 \ln 2 \kappa T_a}{M_a c^2}} \quad (5)$$

where T_a and M_a refer to the temperature and mass of the absorbing molecule, (M_s and M_a are the same when the source is a resonance lamp containing the same molecule as the absorbing gas, but in theory need not be the same.)

Equations (1), (2), and (3) can now be combined to give

$$\bar{T}_j = I_{\nu_j^0} \int_{\nu_j^0 - 2(\Delta_s \nu_j)_D}^{\nu_j^0 + 2(\Delta_s \nu_j)_D} \exp \left\{ - \left[\frac{2(\nu - \nu_j^0)}{(\Delta_s \nu_j)_D} \sqrt{\ln 2} \right]^2 \right\} \exp \left\{ - \ell k_{\nu_j^0} \exp \left[- \left(\frac{2(\nu - \nu_j^0)}{(\Delta_a \nu_j)_D} \sqrt{\ln 2} \right)^2 \right] \right\} d\nu \quad (6)$$

The limits on the integrals of Eq. (6) have been changed (from 0 to ∞ in Eq. (1)) to the more practical case for the Doppler profile. Now, assuming there are other absorption lines within the integration limits which might contribute to the measured transmission of the line ν_j , Eq. (3) must be replaced by the expression

$$k_\nu = \sum_i k_{\nu_i^0} \exp \left\{ - \left[\frac{2(\nu - \nu_i^0)}{(\Delta_a \nu_i)_D} \sqrt{\ln 2} \right]^2 \right\} \quad (7)$$

where the summation is over all lines, including the j^{th} line, which have a finite value of the absorption coefficient falling within the integration limits $\nu_- = \nu_j^0 - 2(\Delta_s \nu_j)_D$ to $\nu_+ = \nu_j^0 + 2(\Delta_s \nu_j)_D$. The transmission of the radiation due to the j^{th} source line is now given by

$$\bar{T}_j = I_{\nu_j^0} \int_{\nu_j^0 - 2(\Delta_s \nu_j)_D}^{\nu_j^0 + 2(\Delta_s \nu_j)_D} \exp \left\{ - \left[\frac{2(\nu - \nu_j^0)}{(\Delta_s \nu_j)_D} \sqrt{\ln 2} \right]^2 \right\} \exp \left\{ - \ell \sum_i k_{\nu_i^0} \exp \left[- \left(\frac{2(\nu - \nu_i^0)}{(\Delta_a \nu_i)_D} \sqrt{\ln 2} \right)^2 \right] \right\} d\nu \quad (8)$$

The total transmission, \bar{T} , in a particular frequency interval is given by combining Eqs. (1), (2), and (8) and summing over all the emission lines in that interval:

$$\bar{T}_{\Delta\nu} = \sum_j I_{\nu_j^0} \int_{\nu_j^0 - 2(\Delta_s \nu_j)_D}^{\nu_j^0 + 2(\Delta_s \nu_j)_D} \exp \left\{ - \left[\frac{2(\nu - \nu_j^0)}{(\Delta_s \nu_j)_D} \sqrt{\ln 2} \right]^2 \right\} \exp \left\{ - \ell \sum_i k_{\nu_i^0} \exp \left[- \left(\frac{2(\nu - \nu_i^0)}{(\Delta_a \nu_i)_D} \sqrt{\ln 2} \right)^2 \right] \right\} d\nu \quad (9)$$

where the summation over j includes all emission lines which have components falling within the frequency interval of interest, $\Delta\nu$. The transmissivity, t, or fractional transmission in a particular interval is given by

$$t_{\Delta\nu} = \frac{\sum_j I_{\nu_j^0} \int_{\nu_j^0 - 2(\Delta_s \nu_j)_D}^{\nu_j^0 + 2(\Delta_s \nu_j)_D} \exp \left\{ - \left[\frac{2(\nu - \nu_j^0)}{(\Delta_s \nu_j)_D} \sqrt{\ln 2} \right]^2 \right\} \exp \left\{ - \ell \sum_i k_{\nu_i^0} \exp \left[- \left(\frac{2(\nu - \nu_i^0)}{(\Delta_s \nu_i)_D} \sqrt{\ln 2} \right)^2 \right] \right\} d\nu}{\sum_j I_{\nu_j^0} \int_{\nu_j^0 - 2(\Delta_s \nu_j)_D}^{\nu_j^0 + 2(\Delta_s \nu_j)_D} \exp \left\{ - \left[\frac{2(\nu - \nu_j^0)}{(\Delta_s \nu_j)_D} \sqrt{\ln 2} \right]^2 \right\} d\nu} \quad (10)$$

and again the summation over j includes all lines within the interval of interest, $\Delta\nu$.

2.2 RELATION BETWEEN ABSORPTION COEFFICIENT AND ABSORBING MEDIUM PROPERTIES

The absorption coefficient of a spectral line is related to the population density of the absorbing gas by the equation (Ref. 3)

$$\int_0^\infty k_\nu d\nu = \frac{\pi e^2}{mc^2} N_{J''} f_{J'J''} \quad (11)$$

Eq. (3) can be integrated over the Doppler broadened line to give (Ref. 1)

$$\int_0^\infty k_{\nu_i} d\nu = k_{\nu_i^0} (\Delta_s \nu_i)_D \frac{\sqrt{\pi}}{2\sqrt{\ln 2}} \quad (12)$$

Equating Eqs. (11) and (12),

$$k_{\nu_i^0} = \frac{2e^2 \sqrt{\pi \ln 2}}{mc^2} \frac{N_{J''} f_{J'J''}}{(\Delta_s \nu_i)_D} \quad (13)$$

where e is the charge on an electron, c is the velocity of light, m is the mass of an electron, $f_{J'J''}$ is the oscillator strength of the appropriate absorption line, and $N_{J''}$ is the number density of molecules in the lower state of the molecule corresponding to the i th line. If the absorbing medium is made up of diatomic molecules, then J'' represents a particular rotational-vibrational-electronic state. Furthermore, if the electronic state is the

ground state and the gas is in Maxwell-Boltzmann equilibrium, then $N_{J''}$ is related to the gas density, N_0 , in a definable way. Following Tatum for Hund's case b, (Ref. 5),

$$\frac{N_{J''}}{N_0} = \frac{(2S+1)(2J''+1) \exp \left\{ -\frac{hc}{\kappa T_a} [\mathcal{J}_0 + G(0) + F(J'')] \right\}}{Q_e Q_v Q_r} \quad (14)$$

where S is the spin quantum number, h is Planck's constant, T_a is the temperature of the gas, \mathcal{J}_0 is the term value for the ground electronic state, $G(0)$ is the term value for the ground vibrational state, $F(J'')$ is the term value for the rotational state and Q_e is the electronic partition function given by

$$Q_e = \sum_n 2(2S+1) \exp \left(-\frac{hc}{\kappa T_a} \mathcal{J}_n \right) \quad (15)$$

Q_v is the vibrational partition function given by

$$Q_v = \sum_v \exp \left[-\frac{hc}{\kappa T_a} G(v) \right] \quad (16)$$

and Q_r is the rotational partition function given by

$$Q_r = \sum_{J''} (2J''+1) \exp \left[-\frac{hc}{\kappa T_a} F(J'') \right] \quad (17)$$

At the temperatures of interest herein and for the diatomic molecules of interest, the partition functions may be approximated by (Ref. 6)

$$Q_e = 2(2S+1) \exp \left(-\frac{hc}{\kappa T_a} \mathcal{J}_0 \right) \quad (18)$$

$$Q_v = \exp \left[-\frac{hc}{\kappa T_a} G(0) \right] \quad (19)$$

and

$$Q_r = \frac{\kappa T_a}{hc B_0} \quad (20)$$

where B_0 is the rotational constant for the ground state. Combining Equations (14), (18), (19) and (20) gives

$$\frac{N_{J''}}{N_0} = \frac{hc B_0 (2J'' + 1) \exp \left[-\frac{hc}{\kappa T_a} F(J'') \right]}{2 \kappa T_a} \quad (21)$$

The value for the oscillator strength, $f_{J',J''}$ is given by (Ref. 5)

$$f_{J',J''} = f_{v',v''} \frac{\nu_{J',J''}}{\nu_{v',v''}} \frac{\delta_{J'',J'}}{2(2J'' + 1)(2S + 1)} \quad (22)$$

where $f_{v',v''}$ is the vibrational oscillator strength, $\delta_{J'',J'}$ is the normalized Hönl-London Factor and $\nu_{v',v''}$ is the frequency at the band head. Combining Equations (13), (21) and (22) gives

$$k_{\nu_i^0} = \frac{e^2 \sqrt{\pi \ln 2} hc B_0 \nu_{J',J''} f_{v',v''} \delta_{J'',J'} N_0 \exp \left[-\frac{hc}{\kappa T_a} F(J'') \right]}{2(2S + 1) mc^2 \kappa T_a \nu_{v',v''} (\Delta \nu_i)_D} \quad (23)$$

This equation expresses the absorption coefficient at line center for a Doppler broadened absorption line in terms of the density, N_0 , and temperature, T_a , of the isotropic absorbing medium. Equation (23), when inserted into Eq. (9) or Eq. (10) permits the calculation of the transmission, \bar{T}_j , or the transmissivity, t , through a medium for all the lines in a band.

2.3 SIMULATION OF SPECTRAL BANDS

The method of simulating the output signal from a spectrometer is described fully in Appendix A. The method employs a digital computer in conjunction with an X-Y plotter. The wavelength and the intensity of each spectral line (in emission or absorption) and the spectrometer bandpass function are input to the computer, which calculates the spectrometer output function (usually a triangular function) for that line and stores this information. The program then adds the contributions, at a given wavelength, of all the lines and feeds the resulting intensity to a plotter. The result is a simulated plot of the transmission of the spectral band as a function of wavelength.

3.0 APPLICATION OF THE BAND ABSORPTION TECHNIQUE TO THE NITRIC OXIDE (NO) MOLECULE

The relations developed in the previous section and Appendix A for constructing simulated band transmission spectra for diatomic molecules is generally applicable to the calculation of the transmission through absorbing media. The relations will be applied here to the NO γ -band absorption problem since data already exist for comparison (Refs. 3 and 4) and because of the prominence of NO as a pollutant emission from combustion processes and as a component of real, high enthalpy gas flows.

3.1 DESCRIPTION OF EXPERIMENTAL DATA

A system has been employed previously to obtain transmission data of the (0,0) NO γ -band through absorption cells, in the laboratory (Ref. 3), and through jet engine exhausts (Ref. 4). The system, illustrated in Fig. 2, consists of a resonance lamp source, transmitting and receiving optics, and a spectrometer receiver. The source is a capillary, high voltage (dc), discharge tube through which a 12:3:1 mixture (by volume) of A:N₂:O₂ flows at a pressure ranging from 1 to 10 Torr. In the laboratory, a 1-meter Czerny-Turner mount spectrometer was used in second order to obtain the spectrum of the source (Fig. 3). Resolution of the instrument was 0.03Å and the slit function was triangular. A number of lines in the spectrum of Fig. 3 could be resolved, and the transmission through absorption cells was measured for the individual lines (Ref. 3). For the resolved lines, Eq. (6) can be employed directly to determine the

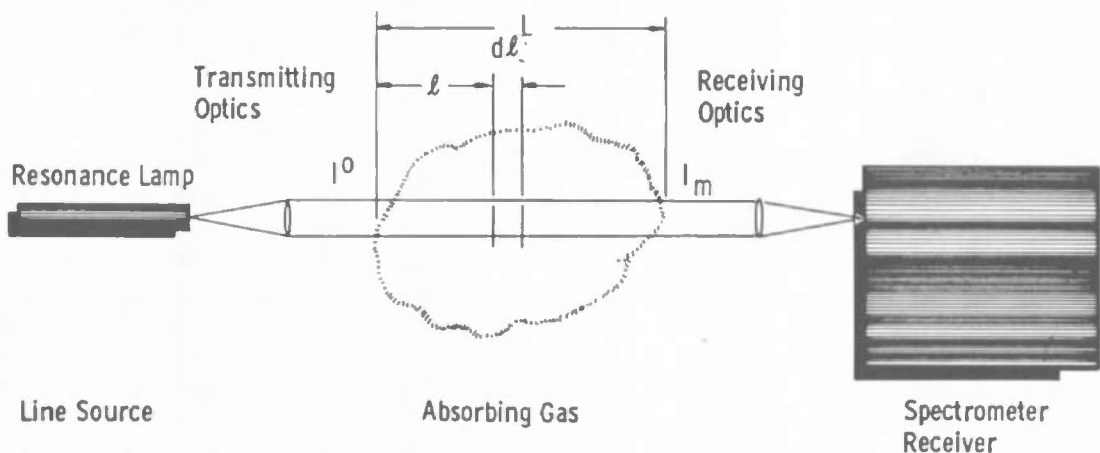


Figure 2. Illustration of physical arrangement for spectral line absorption measurements.

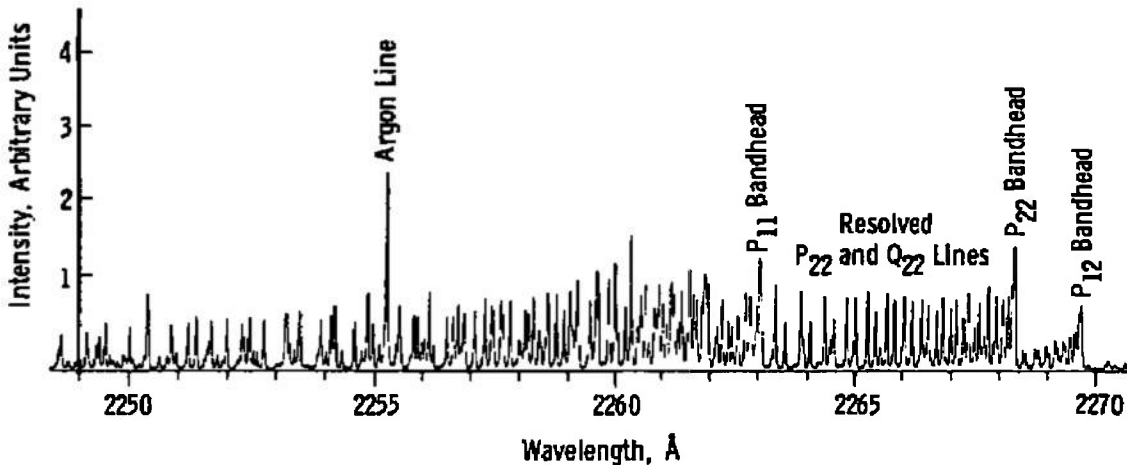


Figure 3. (0,0) Band of the NO γ -system obtained from discharge tube containing a mixture of 12:3:1 (by volume) of A: N_2 : O_2 at 8 torr with 2800 volts applied by use of 1-meter spectrometer in second order (equivalent slit width, 0.03\AA).

absorption coefficient at line center from the measured transmission, and Eq. (23) is used to convert the absorption coefficient to NO number density. For the jet engine exhaust measurements (Ref. 4) it was not possible to use the 1-meter spectrometer employed to obtain the resolved spectra of Fig. 3, and a 1/2-meter Ebert instrument was employed. Resolution of the lines could not be accomplished using the 1/2-meter instrument; an alternative was to open up the slits to obtain a smooth band profile. The emission profile of the NO (0,0) γ -band from the source for an equivalent slit width of 1.6\AA obtained from the 1/2-meter instrument is shown in Fig. 4. The slit function of this instrument was shown to be triangular by examination of the 4158\AA argon line. The spectrum and intensity were repeatable and stable over long periods of time and for successive runs.

The utility of the overlapping, unresolved band treatment (Section 2.0) begins now to become apparent. In the work involving absorption measurements through jet engine exhausts (Ref. 4), a laboratory calibration was made by obtaining the transmission of the NO (0,0) γ -band through the absorption cell which contained pure NO at room temperature for several different pressures. The band spectra obtained are shown in Fig. 5, and a calibration curve of transmissivity at the peak of the second bandhead (corrected to line center transmissivity at room temperature by the method described in Ref. 3) versus the optical path length ($N_0 \ell$) was obtained. This procedure was conceptually unsatisfactory because of the difference in temperature and pressure of the absorber in the case of the jet

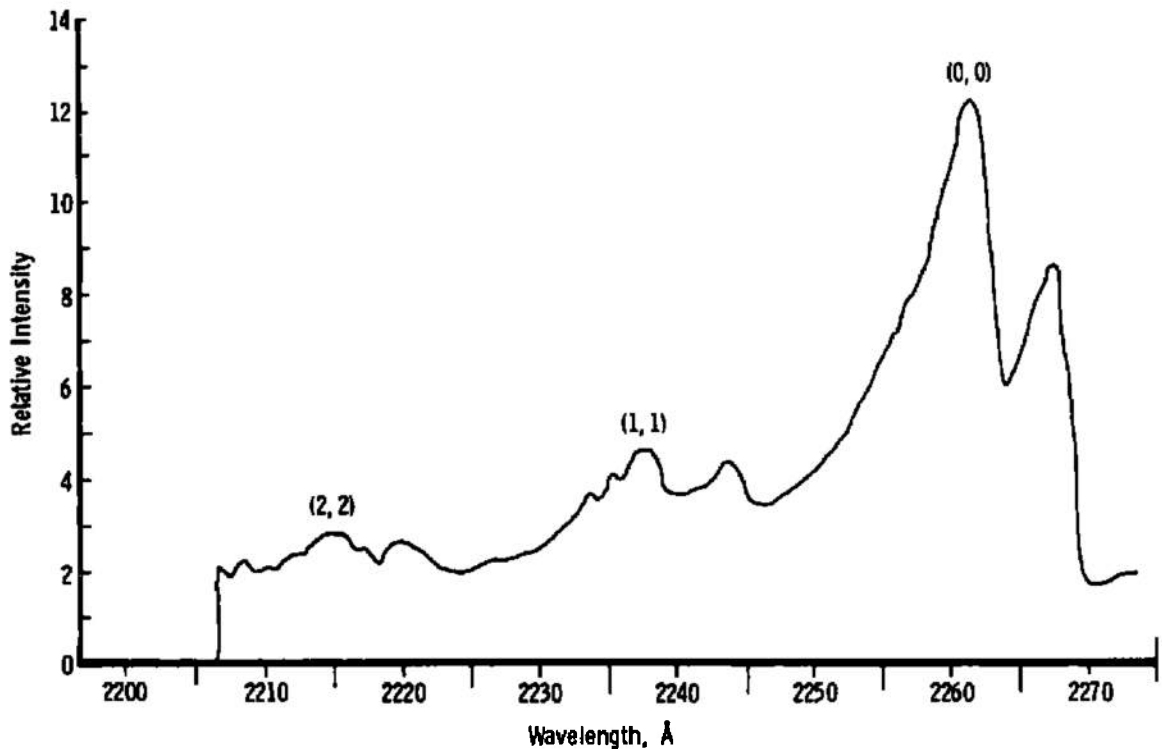


Figure 4. (0,0) Band of the NO γ -system obtained from discharge tube containing a mixture of 12:3:1 (by volume) of A: N_2 : O_2 at 8 torr with 2800 volts applied by use of 1/2-meter spectrometer in first order (equivalent slit width, 1.6Å).

engine exhausts from the calibration case. However, no computational procedure existed for determination of the NO concentration from transmission measurements of the low resolution band spectra, so that the use of the calibration procedure was imperative. In the reduction of the engine exhaust absorption data, a Doppler broadening profile of the absorption lines was assumed and the transmission at the second bandhead was corrected to a "line center" transmission using the method described in Ref. 3. The Doppler assumption was considered valid since the engine exhaust static pressures ranged from 0.05 to 0.2 atm. This procedure produced results which appeared reasonable and consistent. However, it was later recognized that more confidence could be placed in results obtained by using a procedure based on first principles, as developed in this report.

3.2 SOURCE CHARACTERISTICS

A schematic of the resonance lamp used as a line source is presented in Fig. 6. Radiation emerges from either end of the water-cooled capillary tube and is directed through the

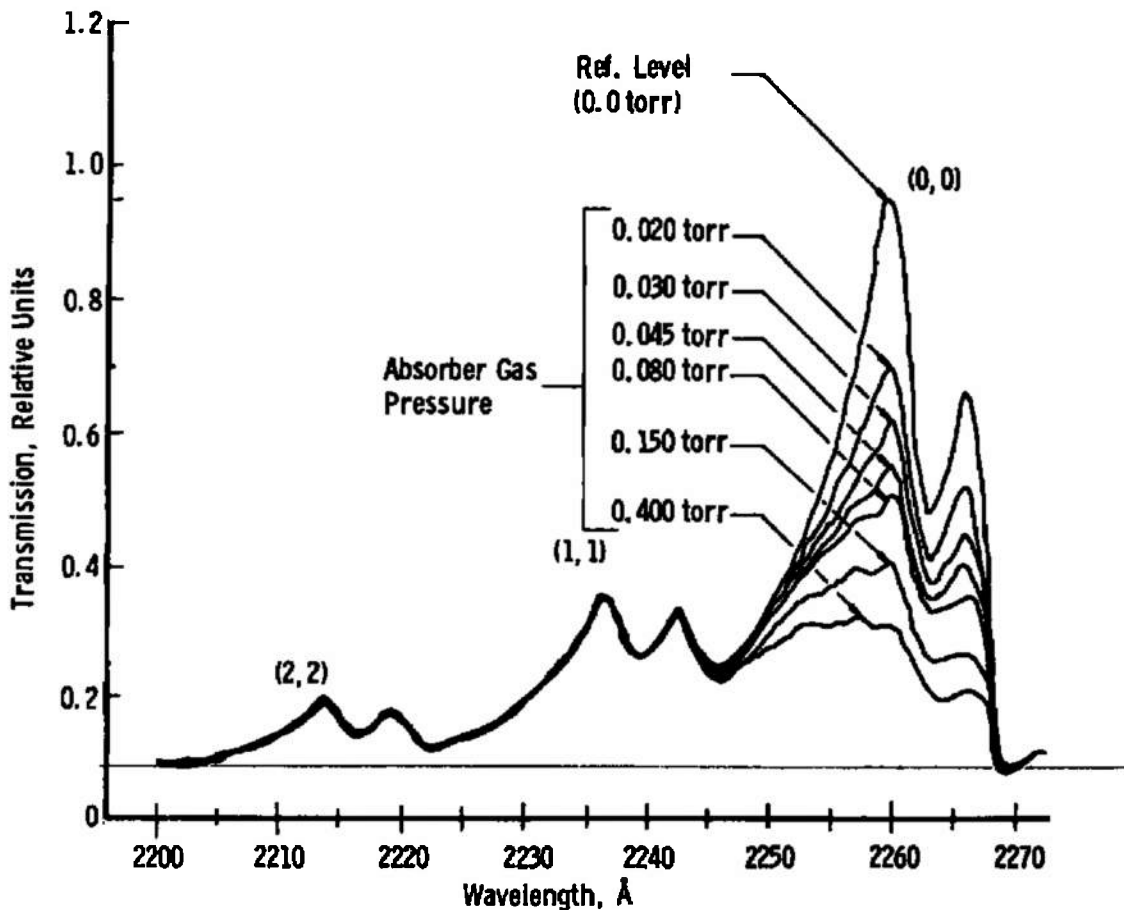


Figure 5. Measured spectral (bandpass — 1.6\AA) profile for transmission of the (0,0) band of the NO γ -system through 300°K NO at selected values of gas pressure and a fixed path length (44.1 cm) from a gas discharge tube containing a 12:3:1 mixture (by volume) of A: N_2 : O_2 and operating at 8 torr with 2800 volts applied and estimated temperature of 320°K .

absorption cell and into the optics of the spectrometer (Fig. 2). The gas temperature in the water-cooled capillary tube is maintained at 320°K . It is assumed that the dominant broadening mechanism under these conditions is due to the Doppler effect. The Doppler line width (Eq. (4)) for the lines of the 0,0 γ -band at 320°K is 0.005\AA , so that the use of a delta function for the lines emitted by the discharge tube is certainly valid for $\Delta\lambda_x = \Delta\lambda_e = 1.6\text{\AA}$, and the convolution integral (see Appendix A) is decoupled.

In order to employ the computational technique developed in Section 2.0, it is necessary to define the relative intensity of each line in the band. Using all the resolved lines

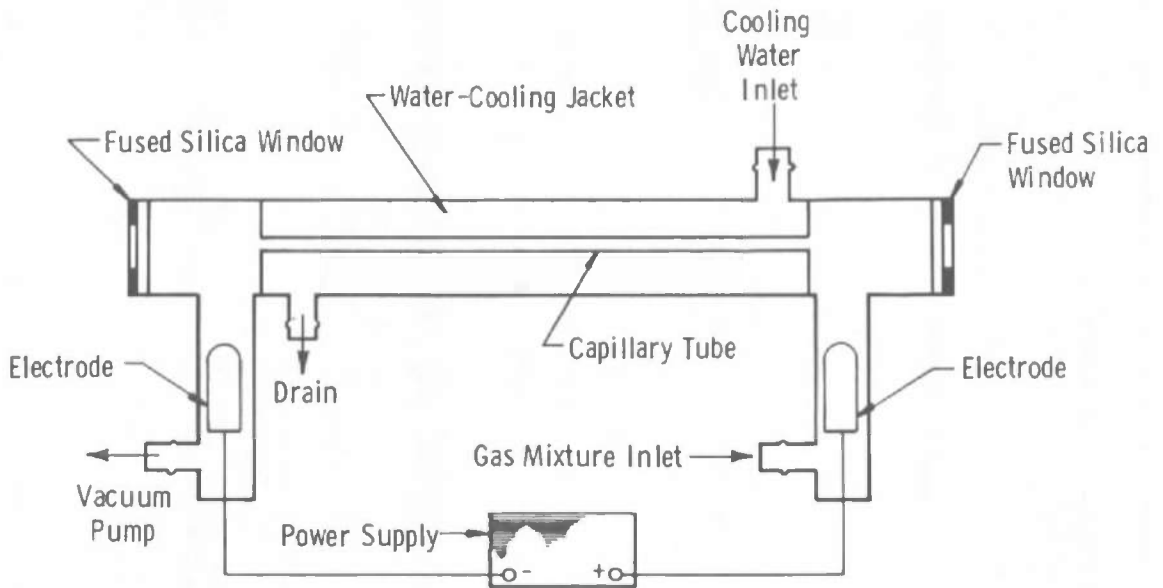


Figure 6. Diagram of resonance lamp used to produce narrow-line radiation.

from the NO spectra of Fig. 3, a plot of $\ln(I_{\nu_j^0}/\delta_{J'J''})$ versus F_{u_j} is made (Fig. 7). F_{u_j} is the rotational energy of the upper electronic state, $A^2\Sigma$, for the j^{th} transition. The plot ranges from $J' = 1/2$ to $81/2$ for the lines that can be resolved. A straight line plot would be indicative of a Boltzmann distribution. It is evident that a Boltzmann distribution cannot be used to express the population distribution of upper states in the discharge tube in this case; therefore, a rotational temperature cannot be defined. In order to find the relative intensity of those lines that are not resolvable, it is necessary to refer to Fig. 7. For a particular line, the value of $I_{\nu_j^0}/\delta_{J'J''}$ corresponding to its value of F_{u_j} , is found from Fig. 7. The value of $I_{\nu_j^0}/\delta_{J'J''}$ is then multiplied by the appropriate value of $\delta_{J'J''}$ resulting in a value of the relative intensity, $I_{\nu_j^0}$, for the $J'J''$ line. Values for $\delta_{J'J''}$ are obtained from the formulae developed by Earls (Ref. 7) as given in Ref. 3.

Experimental values of ν_j^0 , as given by Deezsi (Ref. 8), were used in these calculations. The experimental values of ν_j^0 are more accurate than can be calculated using the Hill and Van Fleck formula (Ref. 6) as discussed in Ref. 3.

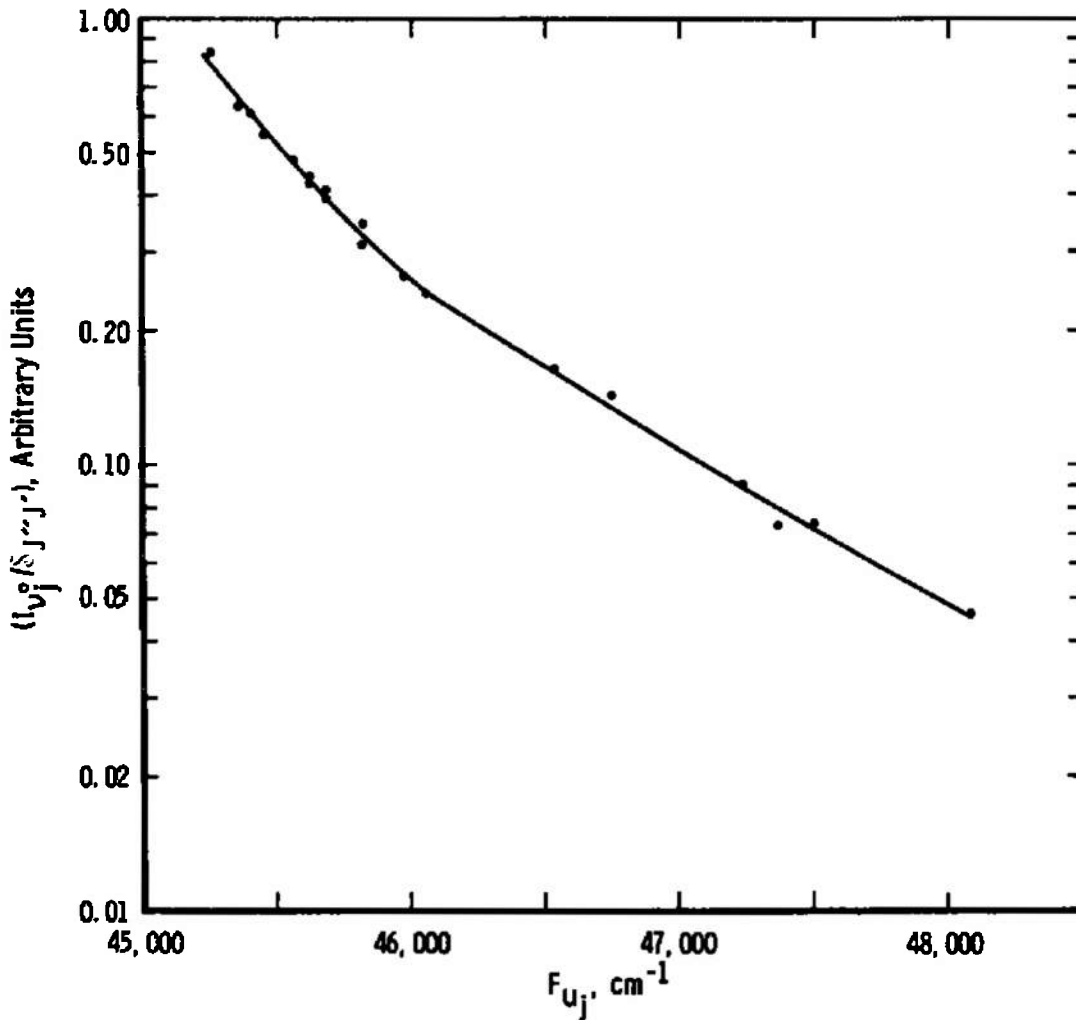


Figure 7. Population distribution of excited rotational states of the $A^2\Sigma$ level of NO in a water cooled discharge tube operated at 8 torr with 2800 volts applied and containing a 12:3:1 mixture (by volume) of A:N₂:O₂.

3.3 SIMULATED SPECTRAL CALCULATIONS

The procedure to be used to calculate band transmission profiles is to determine the terms of Eqs. (8) and (23) and then proceed to calculate the intensity of each individual line emitted by the source after absorption by its corresponding absorption line and all adjacent overlapping lines in the medium. The required terms for calculation of the transmission in Eq. (9) are the line widths, $(\Delta_s v_j)_D$ and $(\Delta_a v_j)_D$, and the line center absorption coefficient, $k_{v_1^o}$, which are obtained from Eq. (23). Once the transmission is calculated for each

line, the spectral plot can be constructed as described in Section 2.3 and Appendix A.

Referring to Equations (4) and (5), the values $(\Delta_s \nu_j)_D$ and $(\Delta_a \nu_j)_D$ are:

$$(\Delta_s \nu_j)_D = 1.307 \times 10^{-7} T_s^{1/2} \nu_j \text{ cm}^{-1} \quad (24)$$

and

$$(\Delta_a \nu_j)_D = 1.307 \times 10^{-7} T_a^{1/2} \nu_j \text{ cm}^{-1} \quad (25)$$

For the (0,0) γ -band of NO, the molecular constants are:

$$B_0 = 1.6957 \text{ cm}^{-1} \text{ (Ref. 9)}$$

$$f_{00} = 3.64 \times 10^{-4} \text{ (Ref. 10)}$$

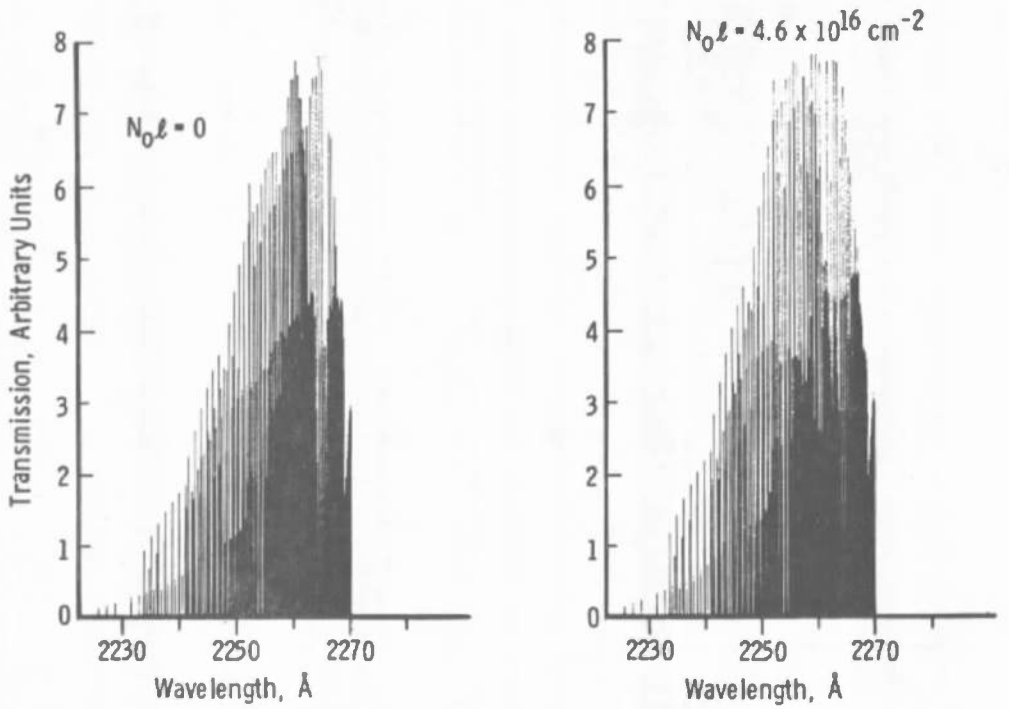
$$\nu_{v'v''} \text{ is } 44065 \text{ cm}^{-1} \text{ (Ref. 8)}$$

Using these values together with Equations (23), (24), and (25) gives for each absorption line, i ,

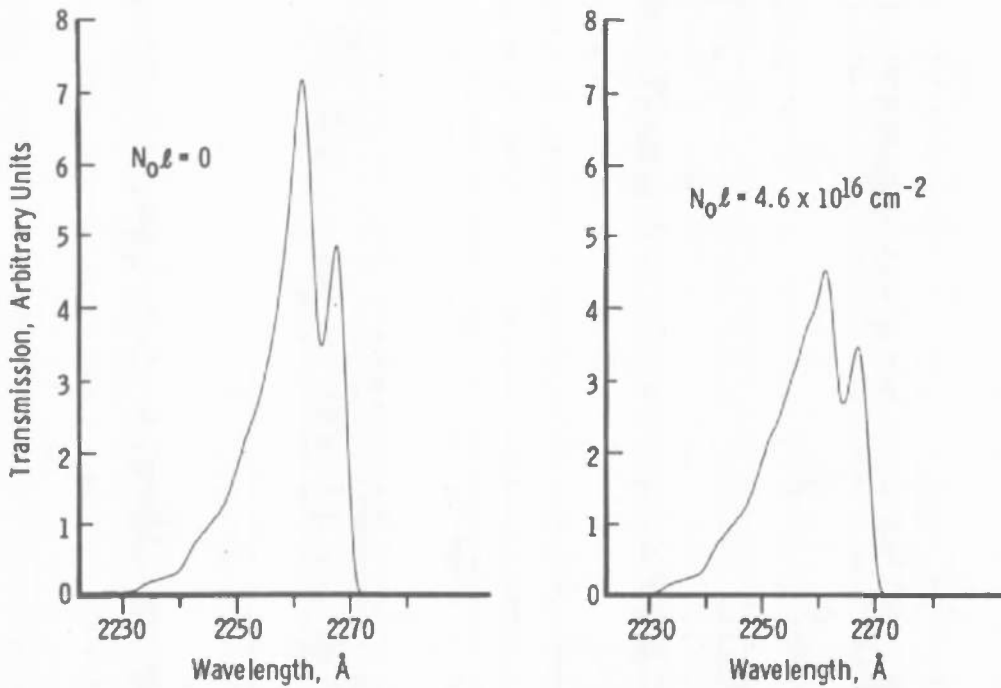
$$k_{\nu_i} = 1.603 \times 10^{-14} \frac{S_J \cdot J'' N_0}{T_a^{3/2}} \exp[-1.4383 F(J'')/T_a] \quad (26)$$

The necessary information is now available to calculate the transmission, \bar{T}_j , for each spectral line, using Eq. (9), for values of N_0 , ℓ , T_s , and T_a . From these calculated line transmissions, and a given value of the spectral band pass of the spectrometer, a computerized spectral plot of the transmitted band radiation can be made. Lines reported by Deeszi (Ref. 8) for J values up to 81/2 are used in the calculations reported herein.

Example high resolution (zero slit width) simulations of the transmission of the (0,0) NO γ -band for $N_0 \ell = 0$ and $4.6 \times 10^{16} \text{ cm}^{-2}$ are shown in Fig. 8a. The computation of the band profile is obtained by forming a triangular function about each line shown in Fig. 8a and then summing the contribution of all the triangles at each wavelength. The result of the summation is shown in the band profiles of Fig. 8b. Spectral plots for various values of $N_0 \ell$ and T_a with a source temperature of 320°K and a spectrometer band pass of 1.6\AA are shown in Fig. 9. From these computed spectra several comparisons with experimental data can be made.



a. Slit width = 0 Å



b. Slit width = 1.6 Å

Figure 8. Illustrative spectral simulation plot for the (0,0) band of NO.

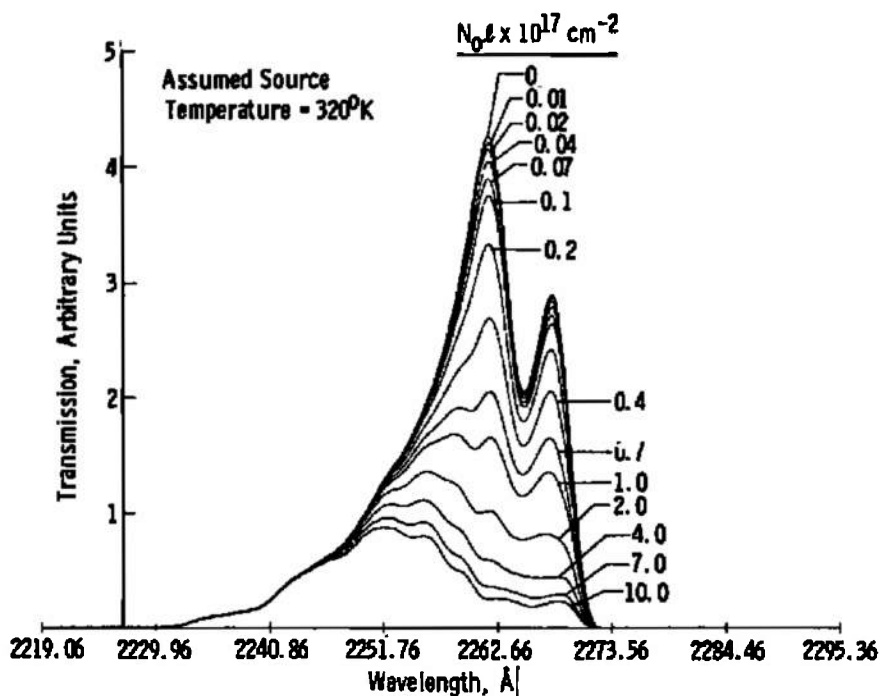
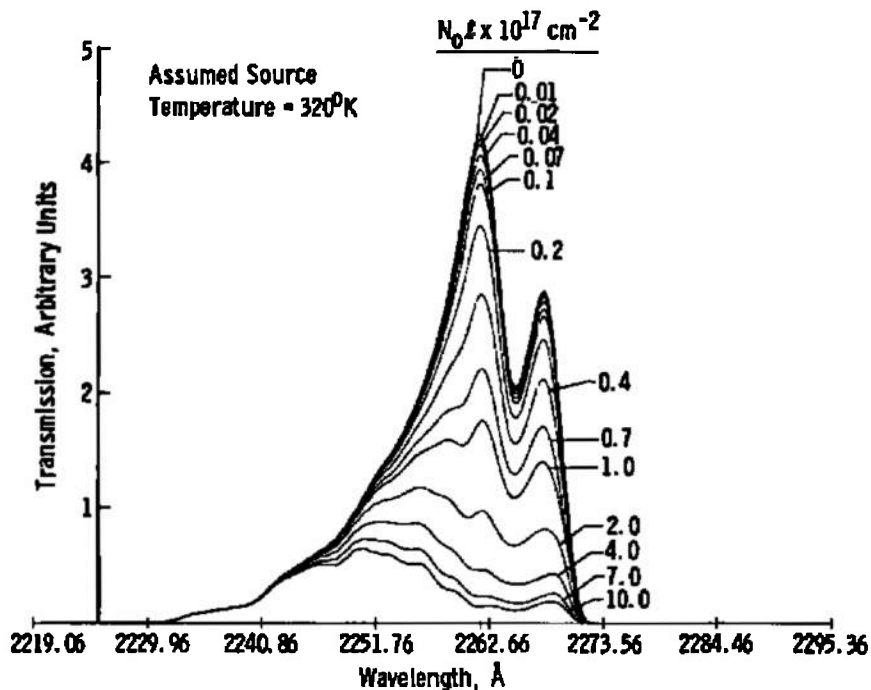
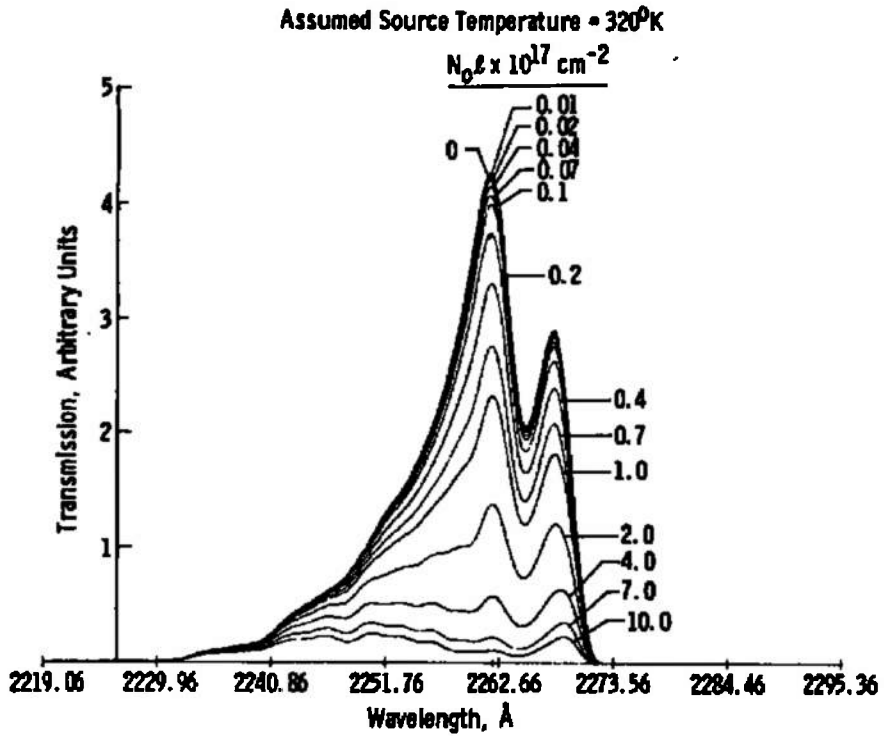
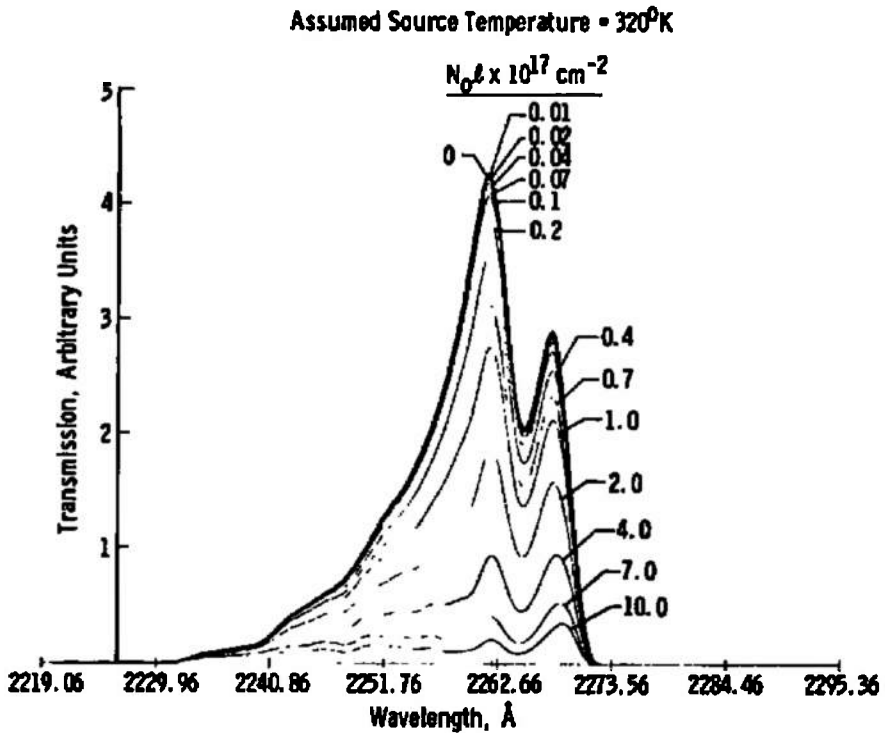
a. Temperature of absorber, $T_a = 300^\circ\text{K}$ b. Temperature of absorber, $T_a = 400^\circ\text{K}$

Figure 9. Calculated spectral plots of the NO (0,0) γ -band corresponding to transmission of radiation from a discharge lamp source containing a 12:3:1 mixture (by volume) of A:N₂:O₂ and operated at 8 torr with 2800 volts applied, through media having several values of the optical path length ($N_o l$).



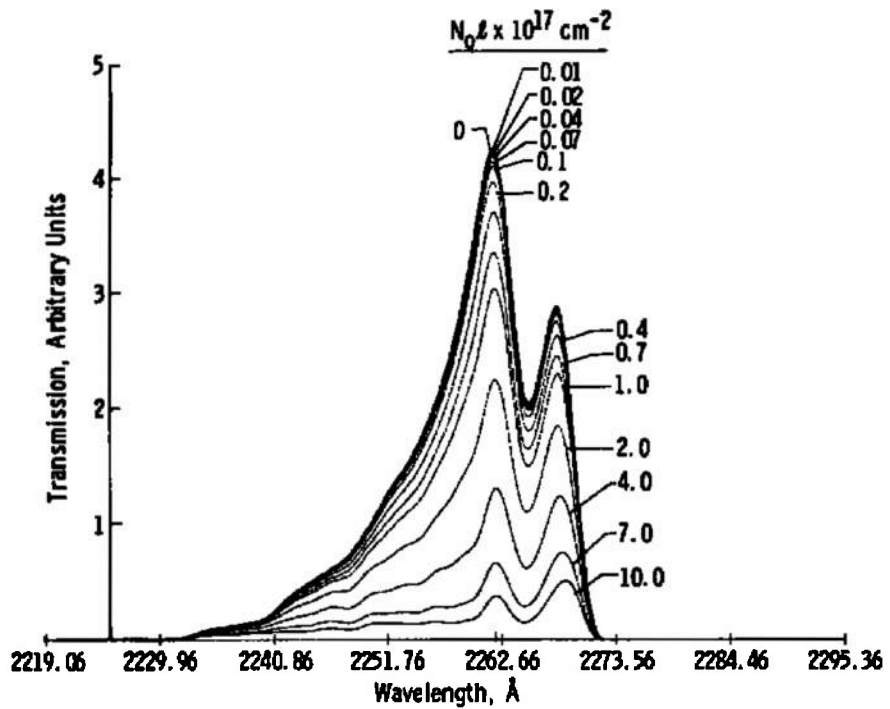
c. Temperature of absorber, $T_a = 800^\circ\text{K}$



d. Temperature of absorber, $T_a = 1200^\circ\text{K}$

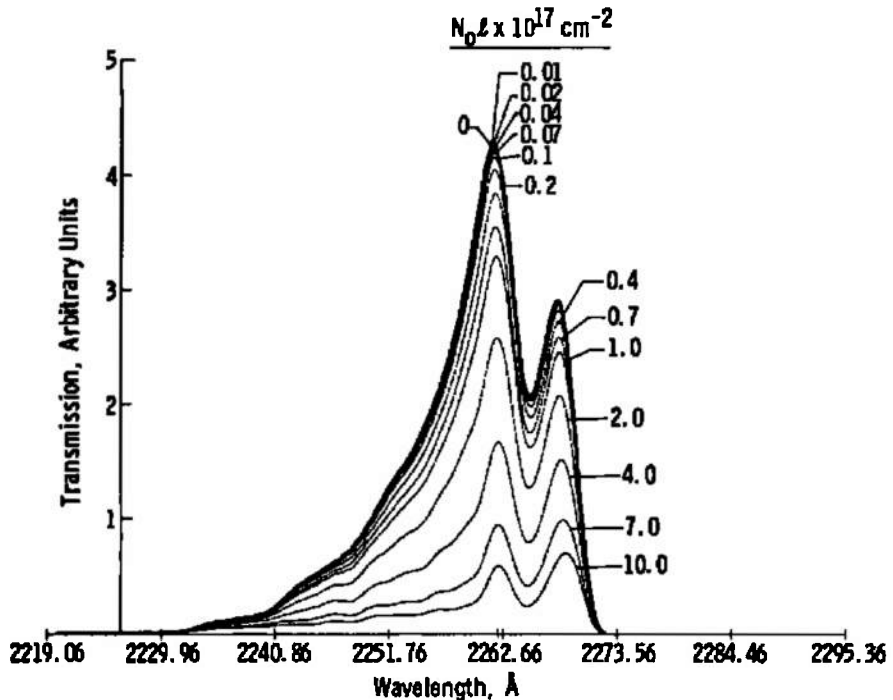
Figure 9. Continued.

Assumed Source Temperature = 320°K



e. Temperature of absorber, $T_a = 1600^\circ\text{K}$

Assumed Source Temperature = 320°K



f. Temperature of absorber, $T_a = 2000^\circ\text{K}$

Figure 9. Concluded.

3.4 COMPARISONS AND APPLICATIONS

3.4.1 Line-by-Line Comparison

The first test of the accuracy of the computation will be made for a single spectral line. In Ref. 3 the theoretical and measured transmissivity were determined for a number of resolved lines in the NO (0,0) γ -band. The calculation procedure used here was tested against the data of Ref. 3 by inputting only one line at a time. Fig. 10 shows the results of the comparison

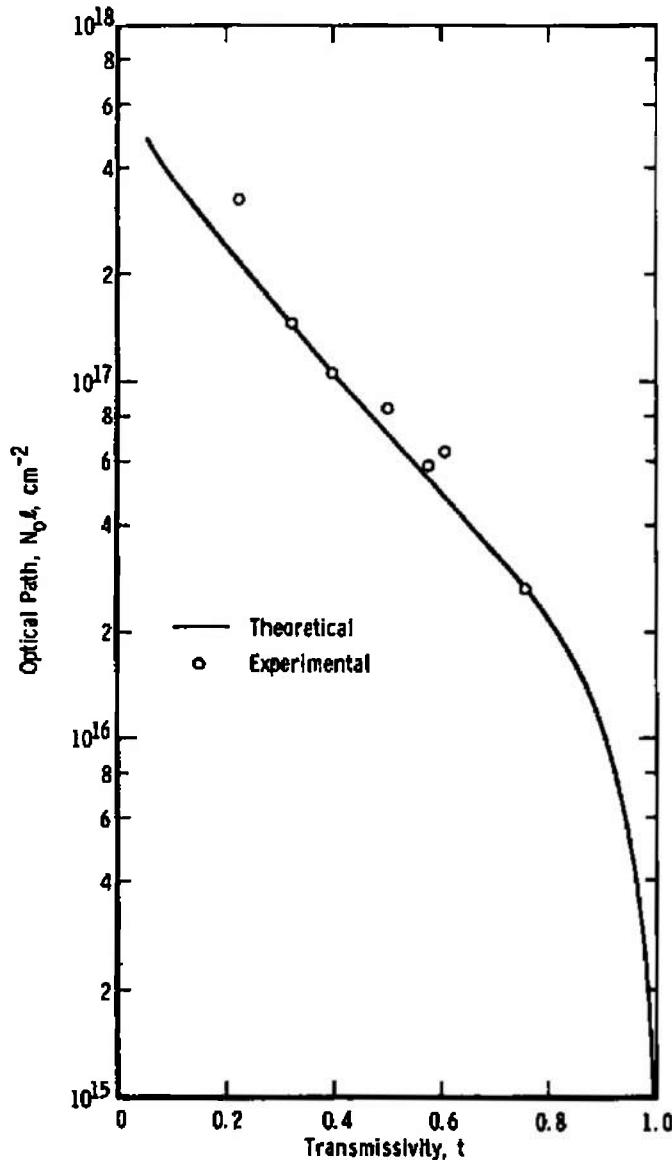


Figure 10. Comparison of measured and calculated transmissivity through pure NO at 300°K as a function of the optical path length ($N_0 L$) for the $Q_{22}(23/2) + R_{12}(23/2)$ line of the (0,0) band of the NO γ -system from a 320°K source.

for the $Q_{22}(\frac{23}{2}) + R_{12}(\frac{23}{2})$ line. The measured data and the theoretical transmissivity as shown in Fig. 10 compare within about ± 6 percent. This agreement serves as a check on the accuracy of both the physical data used in Eq. (32) and the integration procedure used to evaluate Eq. (6).

3.4.2 Spectral Profile Comparison

The band profiles exhibited by the measurements shown in Fig. 5 may be compared with the calculated profiles given in Fig. 11 for the same partial pressure and path length and at $T_a = 300^\circ\text{K}$. The profiles are indeed similar, although the experimental data contain the (0,0), the (1,1), and (2,2) bands while only the (0,0) band is included in the computation so that comparison can only be expected in the (0,0) part of the band. Close examination reveals some discrepancies, particularly at the higher densities. However, for the 0.02-torr partial pressure profile the calculated and measured transmission agree within about ± 3 percent for the entire (0,0) band profile. The experimental values and the theoretical curve of the transmissivity

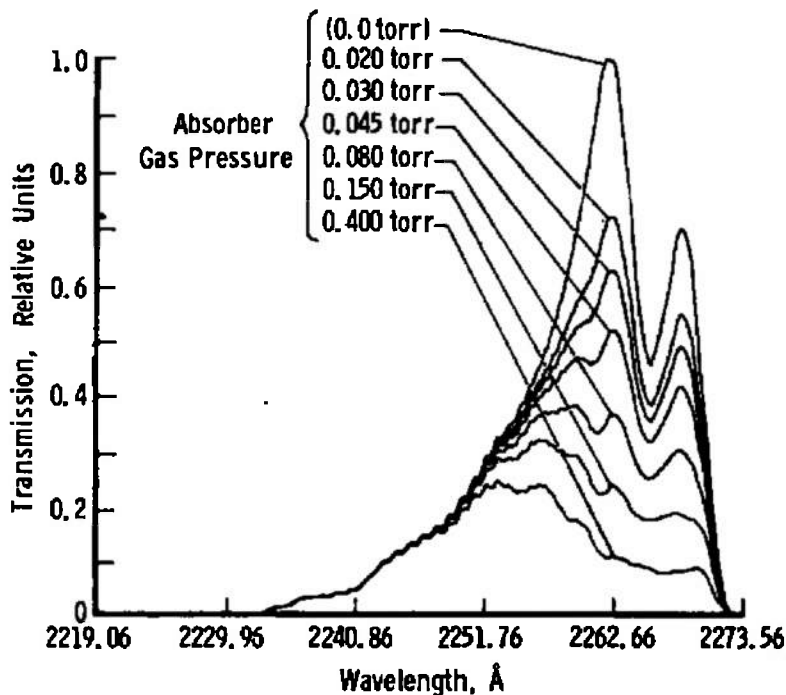


Figure 11. Calculated spectral (bandpass — 1.6 Å) profile for transmission of the (0,0) band of the NO γ -system through 300°K NO at selected values of gas pressure, a fixed path length (44.1 cm), and for a 320°K source with line distribution corresponding to discharge tube pressure of 8 torr and 2800 volts applied.

at the second bandhead (located at 2260\AA) is shown as a function of $N_0 l$ for the $T_a = 300^\circ\text{K}$ case in Fig. 12 and the integrated transmissivity is shown in Fig. 13. The experimental value of the transmissivity at the second bandhead agrees with the theoretical value within about 3 percent up to values of the transmissivity of about 0.5. For $t(2260\text{\AA}) > 0.5$ the departure of the experimental points from the theoretical is quite large and cannot be explained at this time. The differences between the measured and theoretical values of integrated band transmissivity, Fig. 13, are about ± 10 percent over the range studied, but discrepancies at the larger values of transmissivity are smaller than for the second bandhead (Fig. 12).

3.4.3 Calibration for Different Temperatures

The computed transmission data from Fig. 9 are used to obtain transmissivity for the second bandhead ($\sim 2260\text{\AA}$) and for integrated transmissivity over a range of temperatures from 300°K to 2000°K . Plots of the transmissivity at the second bandhead and the integrated transmissivity are shown in Figs. 14 and 15, respectively. These data are useful for the prediction and interpretation of measured band transmission through sources such as jet engine exhausts or wind tunnel flows. The transmissivity at the second bandhead (Fig. 14) is more sensitive than the integrated band transmissivity (Fig. 15) and is more experimentally accessible.

4.0 DISCUSSION

4.1 PROBLEM AREAS AND LIMITATIONS

A technique has been presented for calculation of spectral band profiles as transmitted from a source through a medium of the same substance. The technique is applicable to determination of species density in the medium from measurement of the integrated band transmissivity or the transmissivity at some distinctive wavelength such as an identifiable band peak. Application of the procedure has been made to the $\text{NO } \gamma$ -bands. Several problem areas and limitations in the use of this technique for measuring species densities can be immediately spotted. These limitations include the lack of definition of the line wavelengths and intensities of the source, the detailed line broadening profiles, and the treatment of temperature and density gradients along the absorption path. The limitations imposed by these considerations are discussed in the following sections.

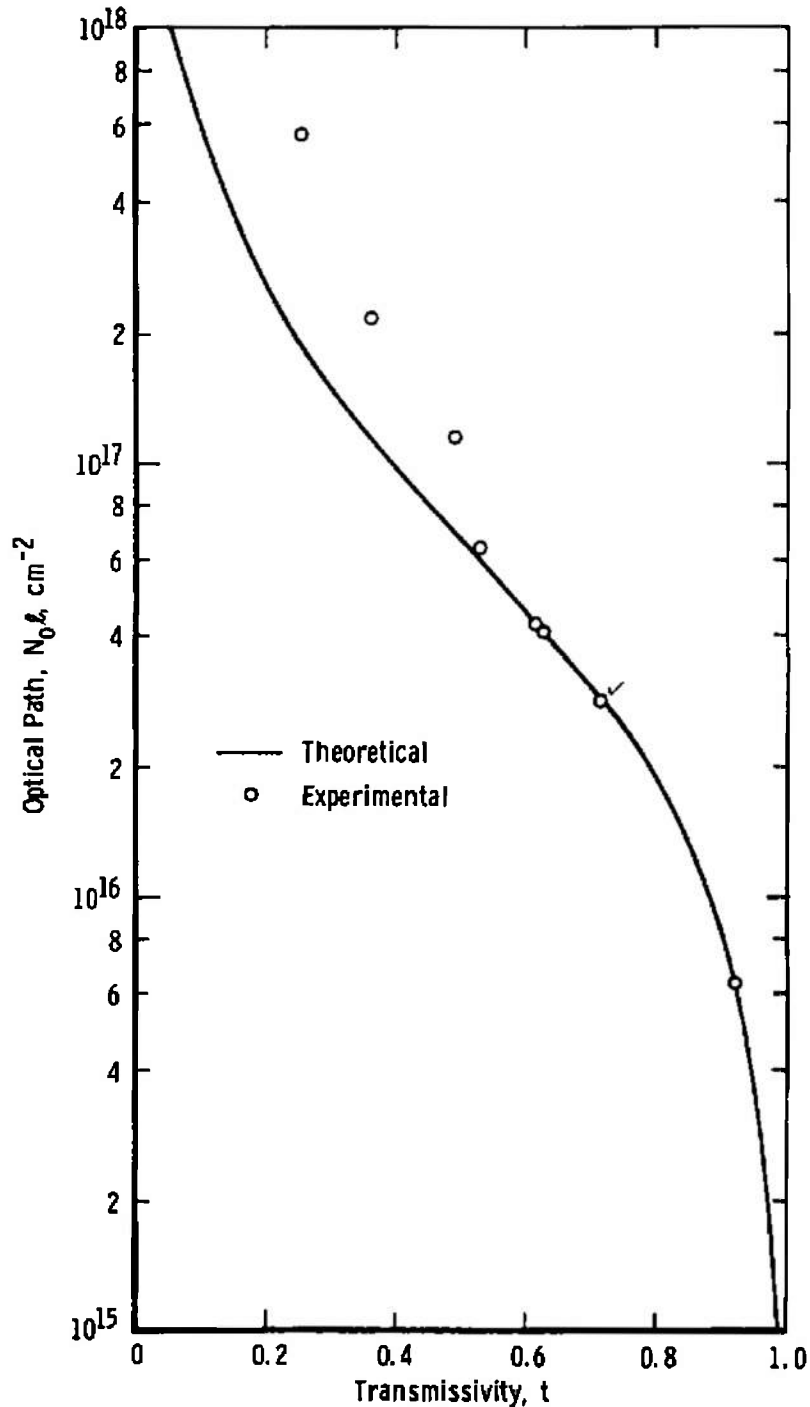


Figure 12. Comparison of measured and computed calibration curves for transmissivity at the wavelength of the second bandhead of the (0,0) band of the NO γ -system versus $N_0 l$ for 300° K absorbing gas, 320° K source gas, and for a source line distribution corresponding to discharge tube pressure of 8 torr and 2800 volts applied.

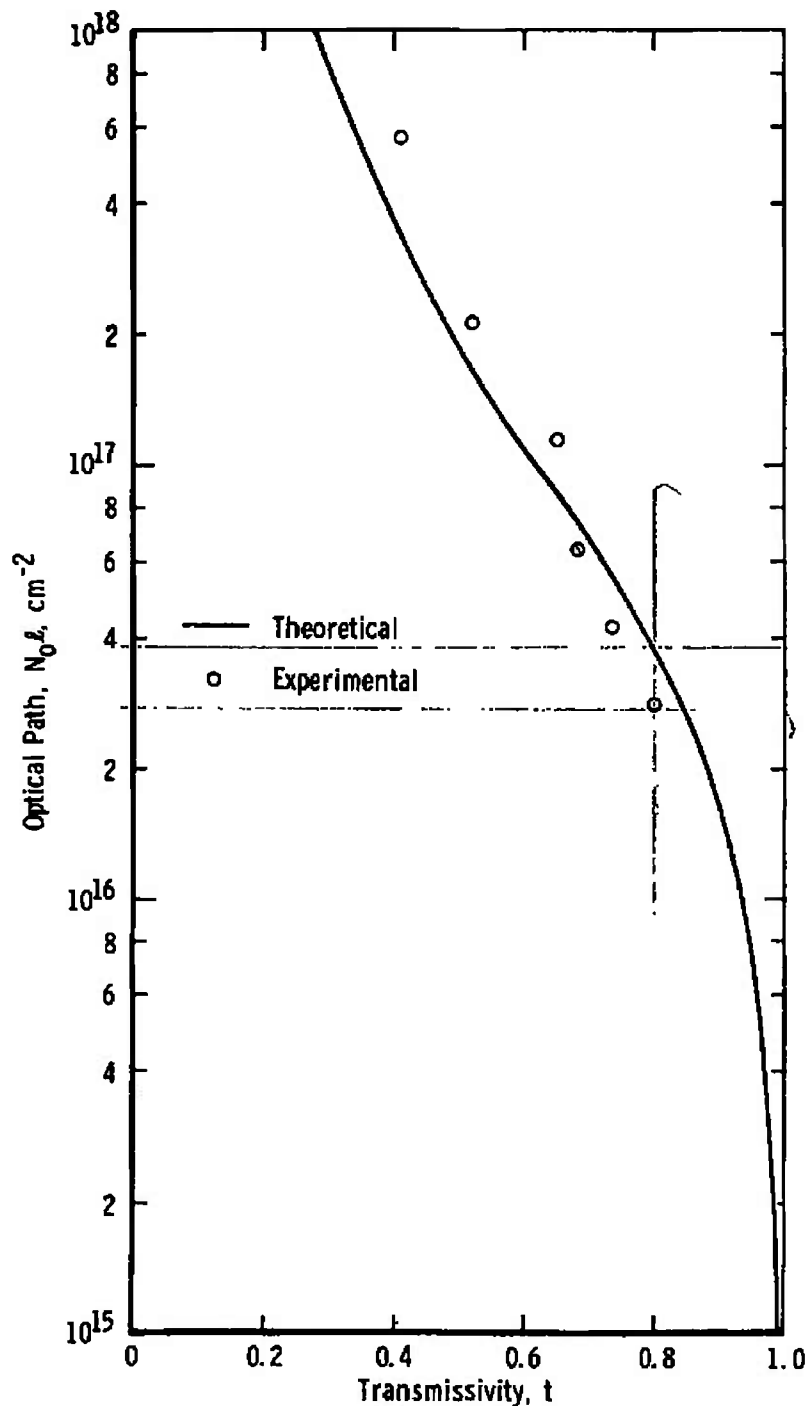


Figure 13. Comparison of measured and computed calibration curves for transmissivity integrated over entire (0,0) band of the NO γ -system versus $N_0 l$ for 300° K absorbing gas, 320° K source gas, and for a source line distribution corresponding to discharge tube pressure of 8 torr and 2800 volts applied.

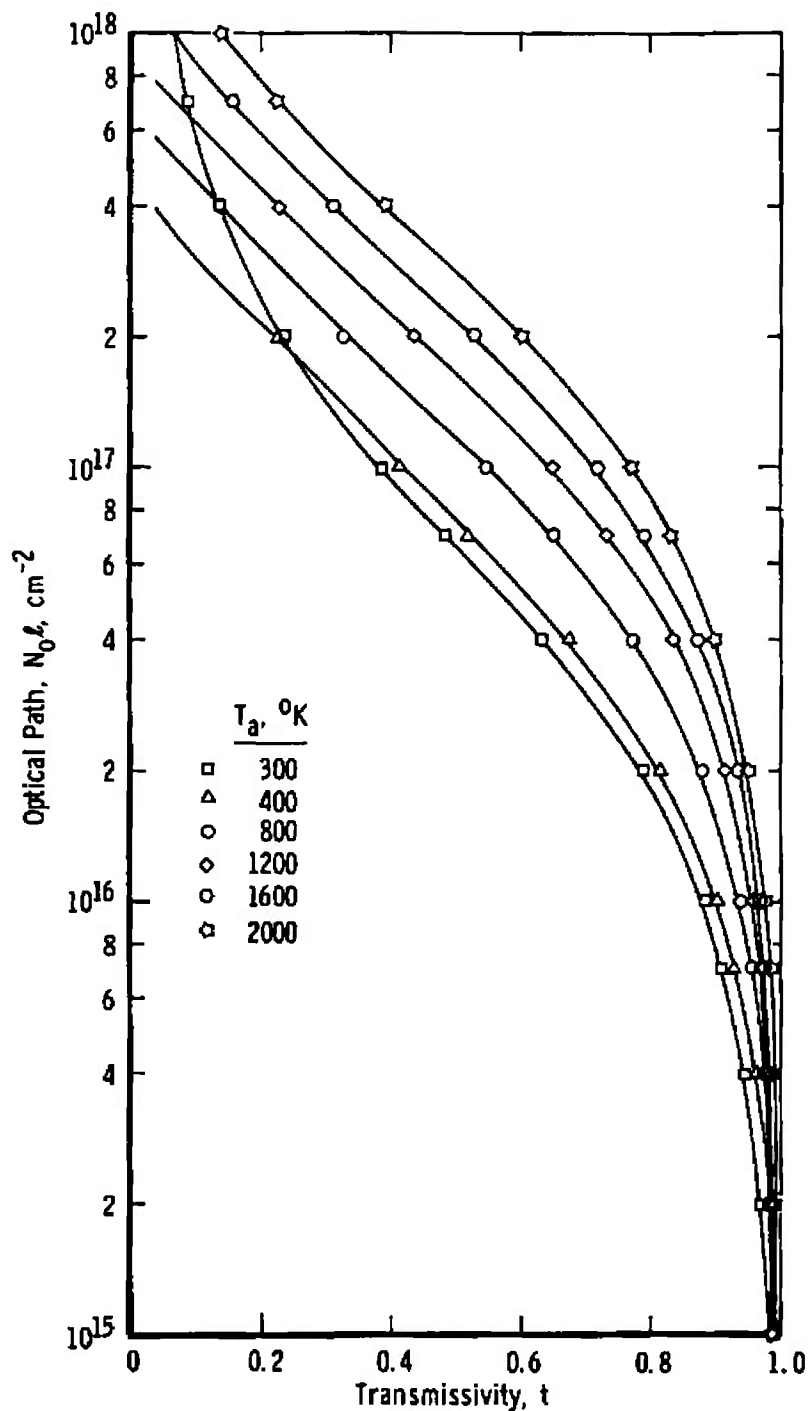


Figure 14. Computed calibration curves for transmissivity at the wavelength of the second bandhead of the (0,0) band of the NO γ -system versus $N_0 l$ with absorber temperature (T_a) as a parameter for 320°K source temperature and a source line distribution corresponding to discharge tube pressure of 8 torr and 2800 volts applied.

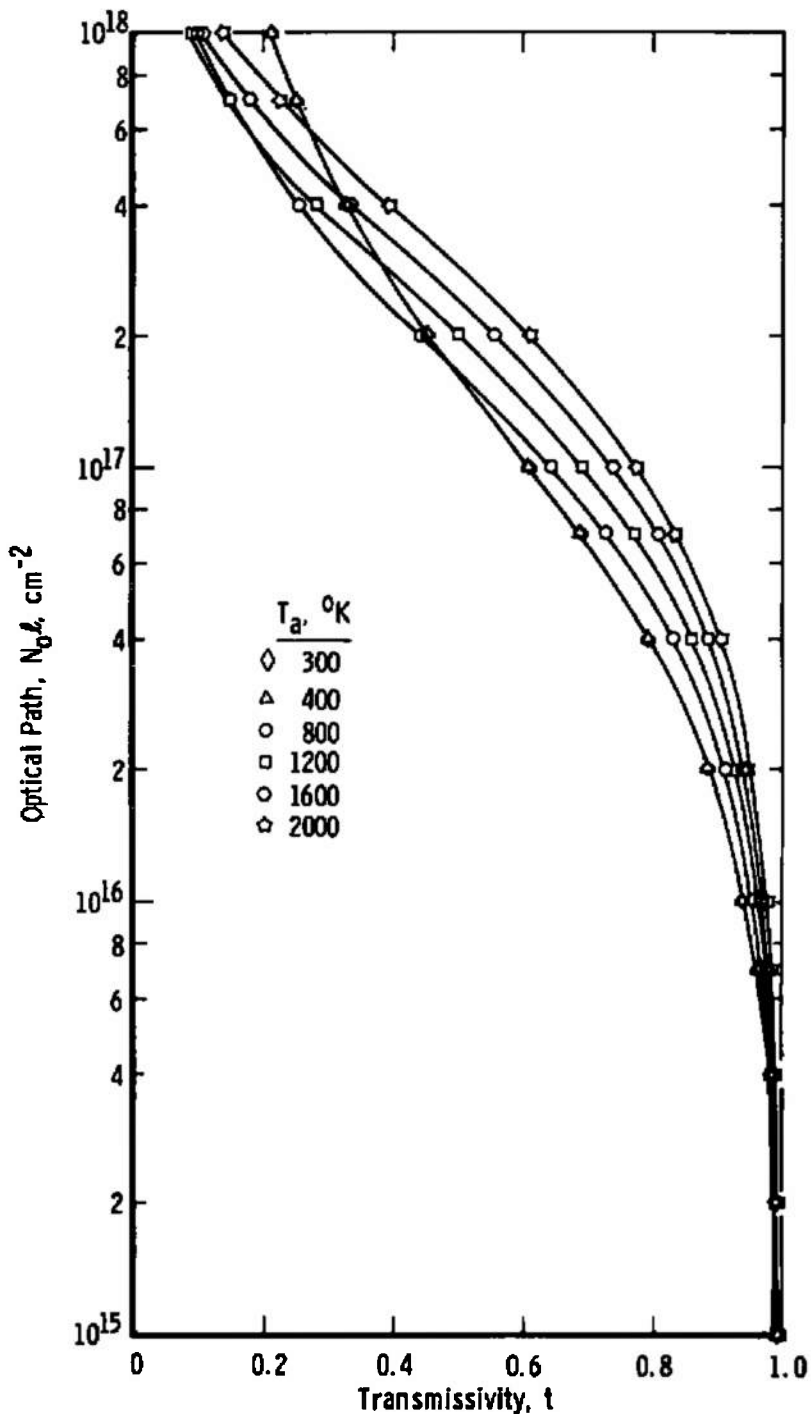


Figure 15. Computed calibration curves for transmissivity integrated over entire (0,0) band of the NO γ -system versus $N_0\ell$ with absorber temperature (T_a) as a parameter for 320°K source temperature and a source line distribution corresponding to discharge tube pressure of 8 torr and 2800 volts applied.

4.1.1 Definition of Source Spectra

The entire computational procedure depends upon definition of the wavelength and intensity distribution of the individual lines from the source lamp. Fundamental knowledge of the molecular structure and molecular constants for the species under study is required. The angular momentum coupling cases of Hund (Ref. 6) and the associated formula for determining energy levels of the individual rotational states are approximations at best and cannot be used indiscriminately to calculate line wavelengths. In the case of the NO molecules, the use of the Hill and Van Fleck formula (Ref. 6) to calculate the wavelengths was not applicable, and the measured line wavelengths of Deezsi (Ref. 8) were used. In the case of at least two other molecules, OH and NH, the inadequacies of analytical expressions to determine wavelengths are well known and the actual wavelengths data are required. For other molecules, the individual situation must be examined. CO may be a particularly nice molecule to work with because of the singlet structure of the ground and resonance state; however, because the resonance transition lies in the vacuum ultraviolet (0,0 band at 1550Å) the use of narrow line absorption for concentration measurements is limited because of instrumentation problems associated with the vacuum ultraviolet spectral region.

The intensity distribution of the lines radiated by a gas discharge source must be measured since they were shown (Section 3.2) to not conform to a Maxwell-Boltzmann distribution (Fig. 7). The determination of the intensity distribution requires measurement of the spectra using an instrument having sufficient resolving power to separate several lines over a wide energy range. The spectral measurement is then used to predict the rotational population distribution of the upper electronic states. Upon first consideration, the distribution of the rotational states might be thought to conform to a Boltzmann distribution. However, the departure of the (0,0) band of NO from a Boltzmann distribution (a straight line) is evident (Fig. 7). The non-Boltzmann distribution might result from the non-equilibrium nature of the electric discharge, or from the excitation collision process involving the argon metastable atom (Ref. 11), or from the recombination process which creates the NO molecule in the A/N₂/O₂ mixture. Another factor which might contribute to the apparent non-Boltzmann distribution is self absorption along the length of the discharge. The latter factor is important, not only because of its effect on the distribution but also because of the non-Doppler line shapes that would result. Since the actual distribution can be measured, no serious limitations result from

the non-Boltzmann distribution, but if the self absorption is a factor then the evaluation of the integral, Eq. (1), should take into account the distorted shape of the lines. The effect of self absorption on the resulting band transmission profiles would be more pronounced at the lower temperatures of the absorbing medium because the two functions, $I_{\nu_j}^0$ and k_{ν_j} , of Eq. (1) have similar half widths. The apparent discrepancy in the calculated and measured band profiles at higher densities in Fig. 11 might result from the self absorption effect on the line profiles.

A high resolution examination of the source spectrum is also necessary to determine if any lines from species other than the one under study are present in the discharge. In the case of the NO (0,0) band, none was found.

4.1.2 Properties of Absorbing Gas

The computation of the transmission through a medium requires knowledge of the population distribution of the states and the properties of the molecule. For chemically inactive media, there is little reason to consider anything other than a Boltzmann distribution of the rotational states. However, care should be exercised in cases where combustion reactions are taking place or where the gas has passed through some non-equilibrium heating phase such as an arc discharge. A major difficulty with the molecular properties may arise in the expression of the rotational line strength factors (the Hönl-London factors), the $\delta_{J',J''}$ of Eq. (23). These factors are determined by assuming a form of the coupling between rotational, orbital, and spin angular momentum which may not be correct. For some molecules, such as OH, experimental line strength data (Ref. 2) are available. For NO it is necessary to use the formulations in the literature (Ref. 3) because experimental data are not available. However, the same coupling scheme is used in determining the line strength relations as in determining the wavelengths by the Hill and Van Fleck formula, which has been shown to be slightly in error for large values of J . Thus, some error in the computation of transmission through NO media is expected due to inadequate values of $\delta_{J',J''}$. The amount of the discrepancy is unknown, but it could account for some of the difference between calculated and measured band profiles shown in Fig. 11.

Another factor which is important in the computation of transmission is the line shape. Throughout the present work, a Doppler broadening profile of the absorber gas was assumed. This assumption was made because the laboratory measurements in this study were made at low-pressure conditions. The

Doppler assumption could not be made at near atmospheric pressure, even for low NO concentrations, where foreign gas collisional broadening will be dominant over self-collisional broadening. It is known that pressure broadening must be taken into account for OH (Ref. 2). For the laboratory studies of Ref. 3, only NO was present in the absorption tube and the pressure was kept at less than 1 Torr so that the pressure broadening was probably not a problem and Doppler profiles as used in this study are adequate. However, in actual applications where the NO is present in only a few hundred parts per million and the pressure is near atmospheric, further study is required.

In the computations considered herein, an isotropic path through the absorbing medium was assumed. If gradients in temperature and concentration are present in the absorbing medium, the procedure for determination of concentration is considerably more difficult. The problem is simplified if the temperature profile along the path is known from some other measurement and if only Doppler broadening must be considered. Further treatment of this case is beyond the scope of the present report.

4.2 UTILITY OF THE METHOD

The determination of concentrations from spectral band transmission measurements can be accomplished, in general, by use of the computational procedure outlined herein. Each specie to be determined must undergo a thorough laboratory and computational study. In the specific case of the NO molecule, the computational method appears to be valid for second band-head transmission over the range of transmissivity from 1.0 down to about 0.5 as evidenced in Fig. 12. In practice, this range of transmissivity corresponds to a range of $N_0 l$ from about 10^{15} (2-percent absorption) to 6×10^{16} molecules/cm². For larger values of $N_0 l$, it will be necessary to use the (0,1) or the (1,1) band of NO (Ref. 3). Further study of the same nature as outlined in this report is required for those bands.

The error in the procedure itself can be estimated from Fig. 12. Over the range of transmissivity from about 0.98 to 0.5 the error should be no greater than about 6 percent. Of course, the conditions of the actual experimental measurement will ultimately determine the error involved in any specific application.

5.0 SUMMARY OF RESULTS

A method of computation of the absorption band profile for diatomic molecules as the profiles would be produced by conventional spectrometers has been developed. A test of the calculation procedure was made by comparison of calculated profiles for the (0,0) γ -band of the NO molecule with existing experimental data. Agreement within about ± 6 percent was found between the calculated and measured transmission at the band maximum for room temperature conditions and pressures less than about 1 Torr and for transmissivity values larger than about 0.5. The calculated results can be used to obtain NO concentration from the measured transmissivity at higher temperatures and pressures so long as the assumption of a Doppler broadening profile is valid. In particular, the transmissivity at the second bandhead of the (0,0) γ -band was found to be useful as a measure of the concentration of NO. The calculations were extended to temperatures that might be encountered in combustion systems, but no comparison could be made with experimental data because such data do not exist for NO absorption. The method was, therefore, satisfactorily demonstrated for the NO molecule at room temperature and low pressure and should be applicable for other diatomic molecules having a resonance absorption spectra such as CO, OH, NH, CH, and CN.

REFERENCES

1. Mitchell, A. C. G. and Zemansky, M. W. Resonance Radiation and Excited Atoms. Cambridge University Press, London, 1971.
- ① 2. Davis, M. G., McGregor, W. K., and Mason, A. A. "Determination of the Excitation Reaction of the OH Radical in H_2-O_2 Combustion." AEDC-TR-69-95 (AD695471), October 1969.
- ② 3. McGregor, W. K., Few, J. D., and Litton, C. D. "Resonance Line Absorption Method for Determination of Nitric Oxide Concentration." AEDC-TR-73-182 (AD771642), December 1973.
- ③ 4. McGregor, W. K., Seiber, B. L., and Few, J. D. "Concentration of OH and NO in YJ93-GE-3 Engine Exhausts Measured in situ by Narrow-Line UV Absorption." Proceedings of the 2nd Conference on the Climatic Impact Assessment Program, Cambridge, Massachusetts, November, 1972.

5. Tatum, J. B. "The Interpretation of Intensities in Diatomic Molecular Spectra." The Astrophysical Journal. Supplement No. 124, March 1967.
6. Herzberg, G. Spectra of Diatomic Molecules. van Nostrand Co., Inc., New York, 1950.
7. Earls, L. T. "Rotational Strength Factors for $2\Sigma \rightarrow 2\Pi$ Transitions." Physical Review. Vol. 48, p. 423, 1935.
8. Deezsi, I. "A Recent Rotational Analysis of the γ -Bands of the NO Molecule." Acta Physica, Vol. 9, p. 125, 1957.
9. Barrow, R. F., and Miescher, E. "Fine Structure Analysis of NO Absorption Bands in the Schumann Region." Proceedings of the Royal Society, Vol. A70, p. 219, 1957.
10. Pery-Thorne, A. and Banfield, F. P. "Absolute Oscillator Strength of the (0,0) Band of the Gamma System of Nitric Oxide by the Hook Method." Journal of Physics B, Atomic and Molecular Physics, Vol. 3, p. 1011, 1970.
11. McGregor, W. K. "Examination of the Conservation Laws in a Particular Class of Collisions of the Second Kind." PhD Dissertation, the University of Tennessee, June 1969.
12. Thorson, W. R. and Badger, R. M. "On the Pressure Broadening in the Gamma Bands of Nitric Oxide", Journal of Chemical Physics, Vol. 27, p. 609, September 1957.

APPENDIX A
METHOD OF SIMULATION OF SPECTRAL BAND PROFILES
FROM REAL INSTRUMENTS

A conventional spectrometer, such as an Ebert mount grating instrument, functions fundamentally by imaging the entrance slit onto an exit dispersion plane such that the image location corresponds to a given wavelength and the image corresponds to a given wavelength interval. If the optics of the instrument are of high quality and the entrance slit is rectangular, then the image will also be rectangular. An exit slit of variable width is placed in the image plane and a detector located behind it, upon which the radiation is made to fall. In order to scan the spectrum, the image plane is made to pass over the exit slit (which may or may not have the same width as the entrance slit). The intensity of the radiation will generally depend upon the wavelength, and thus the imaged radiation in the exit plane will depend upon position in that plane. Let the imaged intensity distribution be represented by $I_{\lambda'}$, where λ' represents the instrument wavelength dispersion in the exit plane; the symbol λ will represent the true wavelength of the radiant source. Now, the radiant power falling on the exit slit is expressed as

$$P \propto \int_{\lambda'_1}^{\lambda'_2} s_{\lambda'} I_{\lambda'} d\lambda' \quad (\text{A-1})$$

where λ'_1 and λ'_2 are the limits of the instrument wavelength interval covered by the exit slit, $\Delta\lambda'_x = \lambda'_1 - \lambda'_2$ and $s_{\lambda'}$ is the instrument slit function.

The apparent intensity distribution, $I_{\lambda'}$, as laid out in the image plane of the spectrometer is now the same as the radiant source intensity distribution, I_{λ} , since at any λ' the apparent intensity is influenced by values of I_{λ} displaced from λ' by as much as $\Delta\lambda'_e$, the equivalent width of the entrance slit. Thus

$$I_{\lambda'} = \int_{\lambda' - \Delta\lambda'_e}^{\lambda' + \Delta\lambda'_e} I_{\lambda} d\lambda \quad (\text{A-2})$$

Putting the integrals (A-1) and (A-2) together, one has a convolution integral of the power received at some wavelength setting, λ'_0 , half way between λ'_1 and λ'_2

$$P_{\lambda'_0} \propto \int_{\lambda'_0 - \Delta\lambda'_e/2}^{\lambda'_0 + \Delta\lambda'_e/2} \epsilon_{\lambda'} I_{\lambda} d\lambda \quad (A-3)$$

Now, $\epsilon_{\lambda'}$, and I_{λ} may be quite complex forms and the integration is not easily performed. Two special cases are immediately apparent, (1) the continuum source in which I_{λ} is a constant, I_0 , and removable from the integration, and (2) the very narrow spectral line compared to the instrument slit width, in which I_{λ} becomes a delta function, $I_{\lambda_0} \delta(\lambda - \lambda_0)$. In the first case

$$P_{\lambda'_0} \propto I_0 \Delta\lambda'_e \int_{\lambda'_1}^{\lambda'_2} \epsilon_{\lambda'} d\lambda' \quad (A-4)$$

and in the second case, if λ'_0 lies within $\Delta\lambda'_x$,

$$P_{\lambda'_0} \propto I_{\lambda_0} \int_{\lambda'_0 - \Delta\lambda'_e/2}^{\lambda'_0 + \Delta\lambda'_e/2} \epsilon_{\lambda'} d\lambda' \quad (A-5)$$

It is this latter case of a monochromatic spectral line that is of most interest here.

Now suppose that I_{λ} is monochromatic as for an infinitely narrow spectral line, that is, I_{λ} has a value only at some λ_0 . Then, the image will be a rectangle with center at λ'_0 and width, $\Delta\lambda'_e$, corresponding to the entrance slit width. Then, the radiant power falling on the detector will be proportional to that part of $\Delta\lambda'_e$ which falls within $\Delta\lambda'_x$. If the spectrometer slit widths are equal and the wavelength setting is at λ'_0 , then $P \propto I_{\lambda_0} \Delta\lambda'_e$. Now suppose there are more than one

monochromatic lines within the wavelength interval $2\Delta\lambda'_x$. Then each line will have an image in the exit plane of width $\Delta\lambda'_e$, and the images will overlap as shown for three spectral lines shown schematically in Fig. A-1. If, in Fig. A-1, the exit slit is the same width as the entrance slit and placed at λ'_b , then energy from all three lines will fall on the detector, and the power received will just be the sum of the intensity of each line times the image area falling on the exit slit. That is,

$$P \propto I_a [\Delta\lambda'_x - (\lambda'_b - \lambda'_a)] + I_b \Delta\lambda'_x + I_c [\Delta\lambda'_x - (\lambda'_c - \lambda'_b)] \quad (A-6)$$

The normal mode of operation of a spectrometer is to pass the exit image plane across the exit slit. The power falling on the detector as a function of position of the image with respect to the exit slit, or wavelength, for a single line for which $\Delta\lambda'$ is just a rectangular function,

$$\Delta\lambda' = \begin{cases} 1 & \lambda'_1 < \lambda' < \lambda'_2 \\ 0 & \lambda' > \lambda'_2, \lambda' < \lambda'_1 \end{cases}$$

can then be expressed as

$$P_{\lambda'} \propto \int_{\lambda'_1}^{\lambda'} I_{\lambda_0} d\lambda' \quad (\text{A-7})$$

$P_{\lambda'}$ can be plotted as shown in Fig. A-2 for a single, monochromatic line. Three cases with the situations (a) $\Delta\lambda'_x = \Delta\lambda'_e$, (b) $\Delta\lambda'_x > \Delta\lambda'_e$, and (c) $\Delta\lambda'_x < \Delta\lambda'_e$ are shown. Note that in each case the maximum height of the detector signal is proportional to the intensity of the line. Also, note that the indicated line wavelength, λ'_0 , is not the true wavelength, λ_0 , in either case. The case of equal exit and entrance slit widths, Fig. A-2a, is the most desirable from an interpretation standpoint and will be the one considered here for spectrometer simulation calculations. For this case the result of the integration is an isosceles triangle of base width $2\Delta\lambda'_e$, and the spectrometer is said to have a triangular slit function.

Suppose now that there are more than one monochromatic lines within $2\Delta\lambda'_x$ as in Fig. A-1 and the spectrometer is being scanned as in Fig. A-2a. Let the intensity of each line be represented by the height of the image as shown in Fig. A-3. Now, one can determine the shape of the indicated, overlapping peak by the construction shown or given the shape of the conglomerate, in principle, the individual line intensities can be determined. An alternate way to arrive at the conglomerate shape is shown in Fig. A-4. Here, a line of height proportional to the intensity is drawn at $\lambda_i + 1/2 \Delta\lambda'_x$ for each spectral line and the triangular slit function of base width $2\Delta\lambda'_x$ formed about that line is constructed. To arrive at the conglomerate profile, the contributions from each line are simply added up. This is the method used in the computer simulation of the spectrometer reported herein. In this way, any number of spectral lines can be included and the band profiles of vibration-rotation bands can be simulated provided knowledge of λ_i and I_{λ_i} exists for

all the lines. Such a construction can of course be made by a computer for slit functions other than triangular.

The case of absorbed lines can also be treated in much the same way as emission lines. The intensity I_λ , in Eq. (A-3) can be replaced by the transmitted intensity of a narrow line, $T_{\lambda_j^0} = I_{\lambda_j^0} \exp(-k_{\lambda_j} l)$. The result of integrating this expression for the case where the width of $I_{\lambda_j^0}$ is much smaller than the equivalent instrument width is still a delta function of the transmission, $\bar{T}_{\lambda_j^0} \delta(\lambda - \lambda_j^0)$, so that the same kind of construction of the conglomerate profiles can be made for lines in absorption as in pure emission.

The computer program functions to first calculate the transmission of each line, $\bar{T}_{\lambda_j^0}$, by use of the transmission expression, Eq. (9), and the absorbing medium properties, Eq. (23), as presented in the main text, and then to calculate and plot the spectrum to be expected from a spectrometer having a given slit function. In the case considered in this work a triangular slit function was used. Imperfections in optics and optical alignment on actual spectrometers cause distortion of the rectangular image so that the triangular pattern is not adhered to at the base and apex of the triangle, but for most work the triangular assumption is adequate.

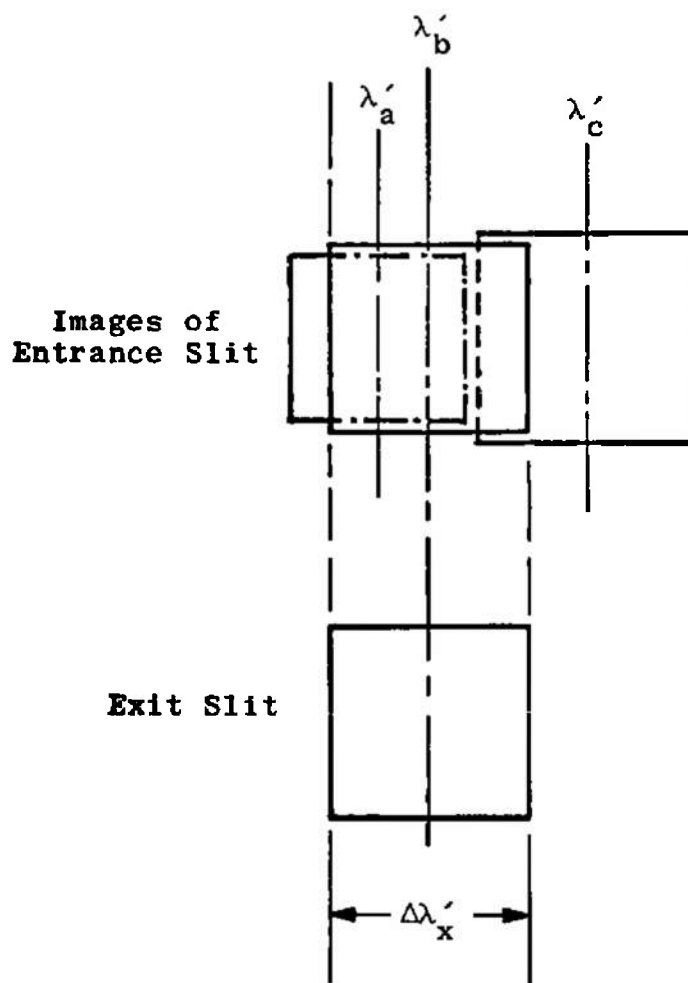
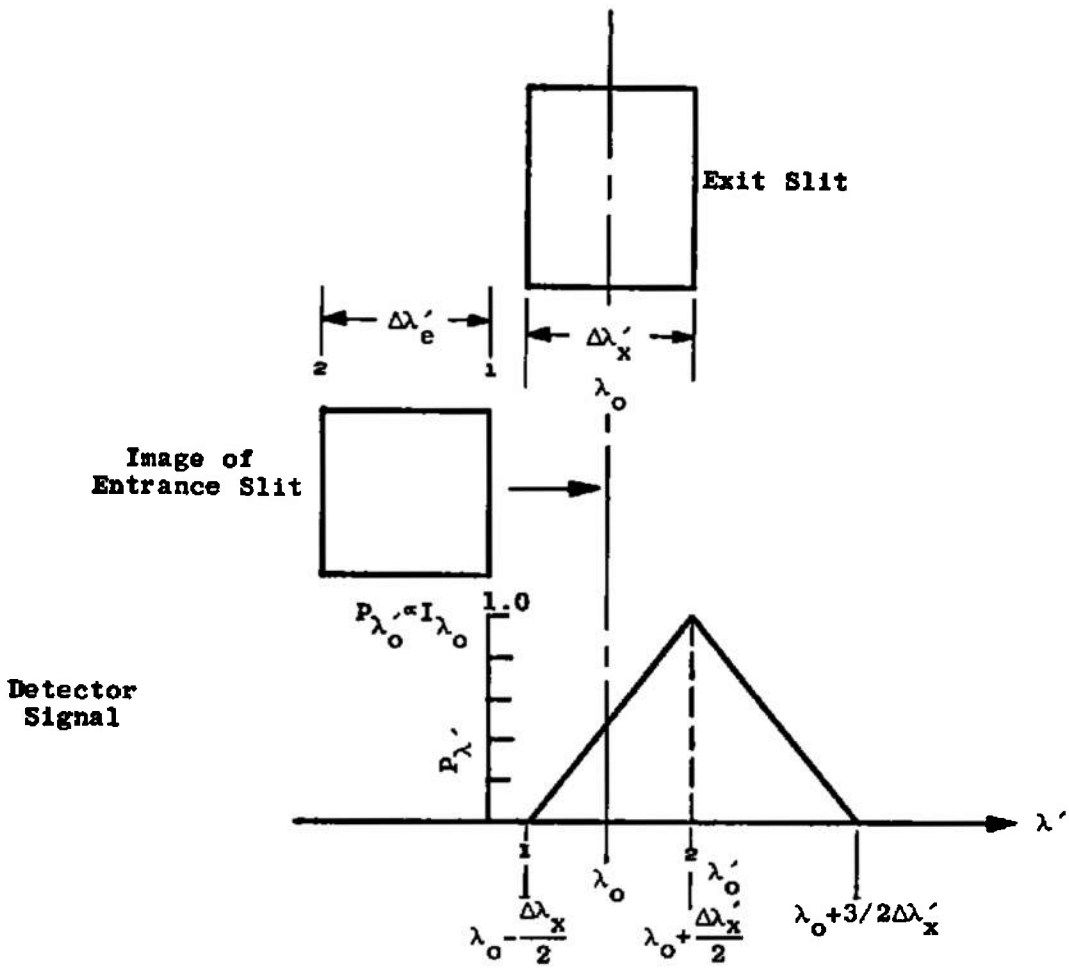
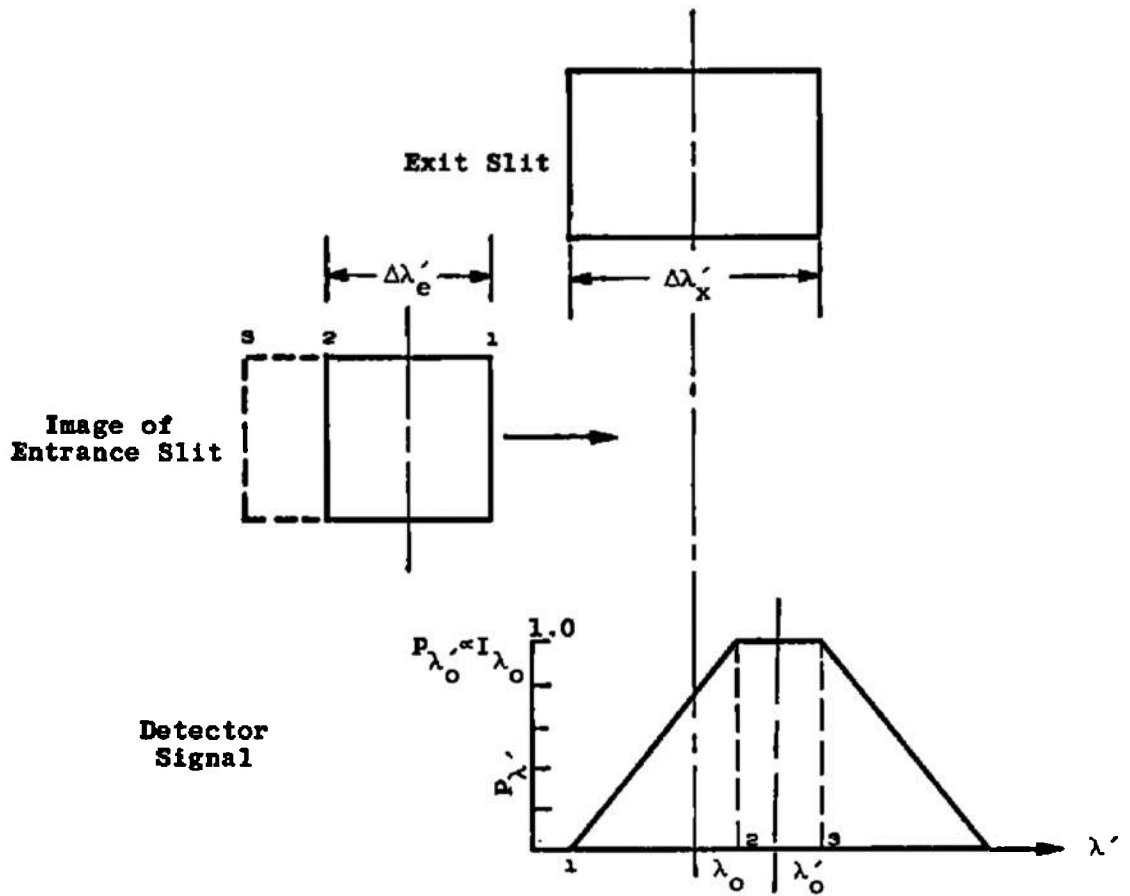


Figure A-1. Image of spectrometer entrance slit for overlapping monochromatic lines.

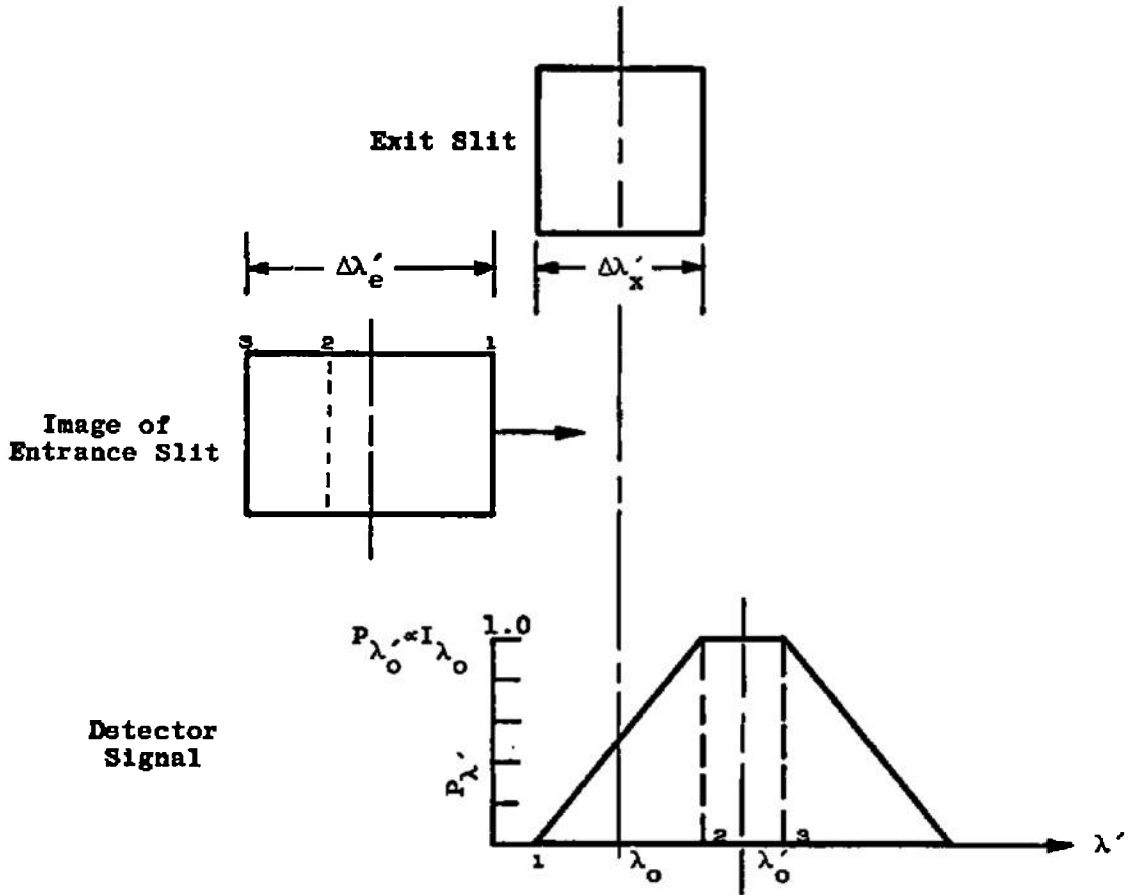


a. $\Delta\lambda'_x = \Delta\lambda'_e$

Figure A-2. Spectrometer slit function for the three possible cases: exit slit width (a) equal to, (b) greater than, and (c) smaller than the entrance slit width.



b. $\Delta\lambda'_x > \Delta\lambda'_e$
 Figure A-2. Continued.



c. $\Delta\lambda'_x < \Delta\lambda'_e$

Figure A-2. Concluded.

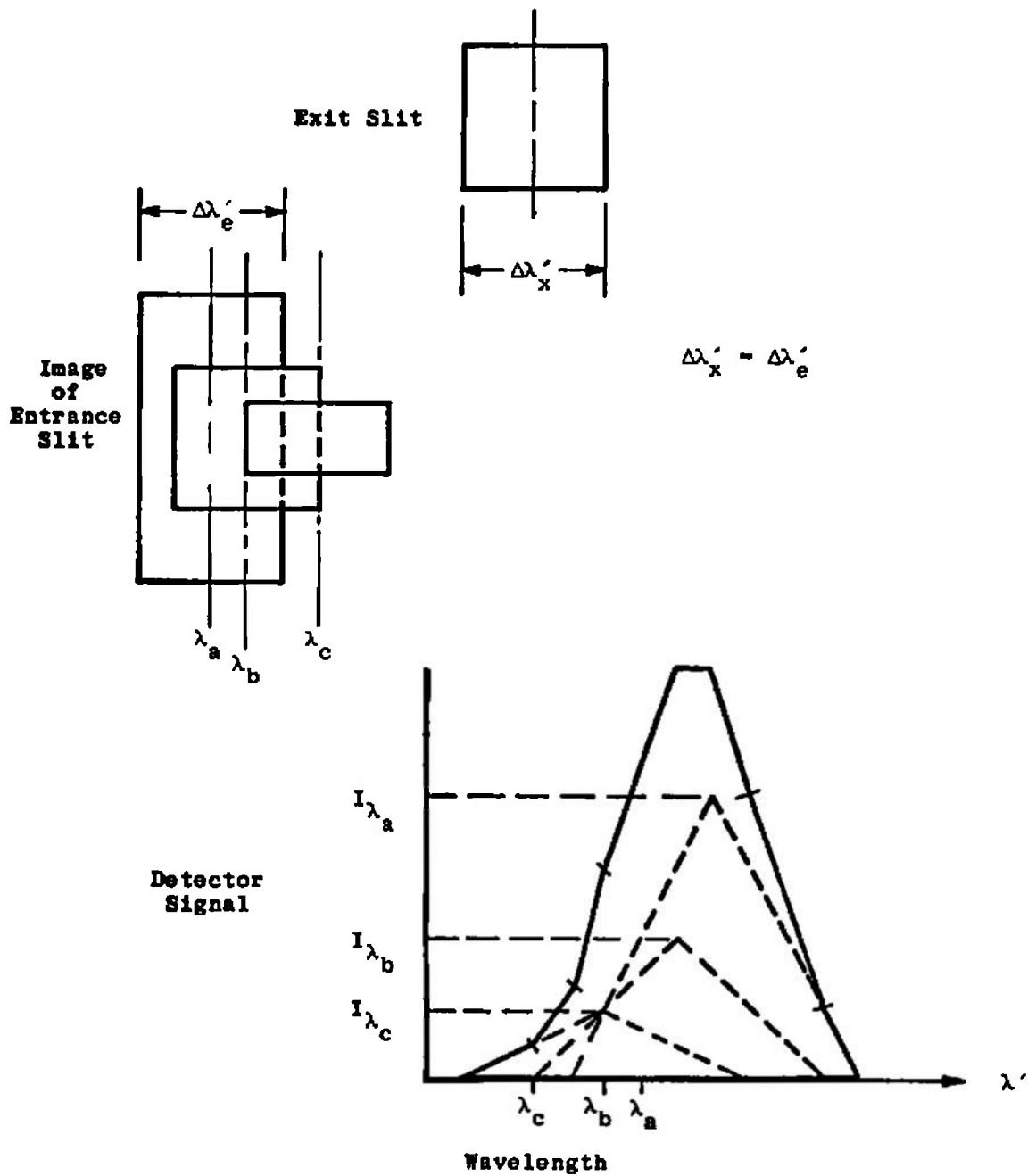


Figure A-3. Construction of conglomerate spectral profile of three overlapping monochromatic lines by passing the image past the exit slit.

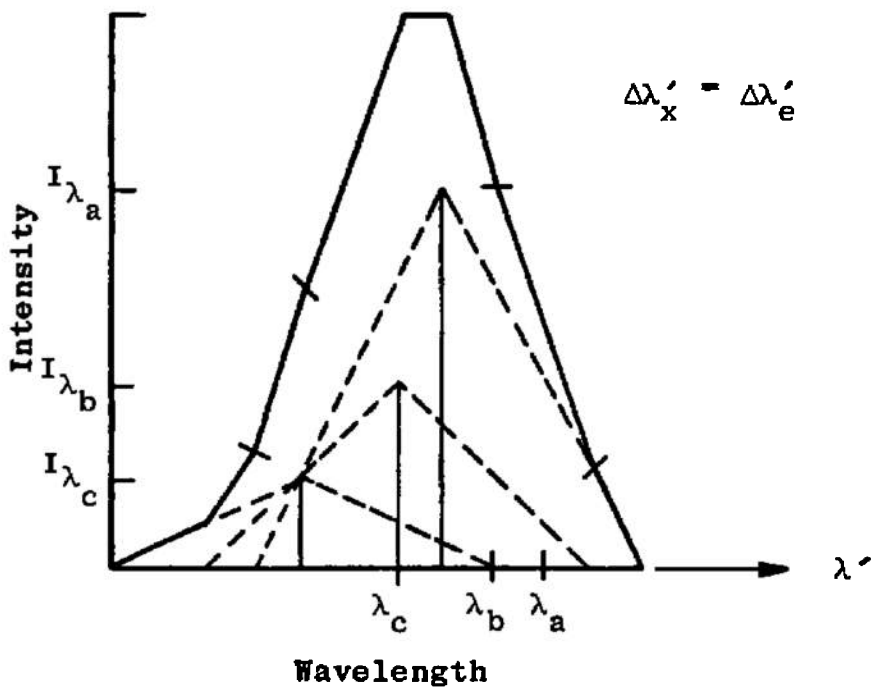


Figure A-4. Construction of conglomerate spectral profile of three overlapping monochromatic lines from knowledge of line intensities, wavelengths and spectrometer slit function.

NOMENCLATURE*

- \bar{T}_j Transmission of spectral line (designated j) through a medium, intensity units
- ② $I_{\nu_j}^0$ Intensity of source spectral line at wavenumber, ν_j , intensity units
- ⑤ k_{ν_j} Absorption coefficient for the spectral line at wavenumber, ν_j , cm^{-1}
- l Absorption path length, cm
- ⑥ ν_i, ν_j Wavenumber of the i^{th} or j^{th} spectral line, cm^{-1}
- ν Wavenumber, cm^{-1}
- ⑦ ν_i^0, ν_j^0 Center wavenumber of the i^{th} or j^{th} spectral line, cm^{-1}
- ⑧ $(\Delta_s \nu_i)_D, (\Delta_s \nu_j)_D$ Doppler width at half maximum intensity of the i^{th} or j^{th} source spectral line, cm^{-1}
- ⑥ $I_{\nu_j^0}^0$ Intensity of source spectral line at center wavenumber, ν_j^0 , intensity units
- $k_{\nu_j^0}$ Absorption coefficient at center wavenumber, ν_j^0 , cm^{-1}
- ⑬ $(\Delta_a \nu_j)_L$ Doppler width at half maximum absorption coefficient, $k_{\nu_j^0}$, of the absorption line, cm^{-1}
- ⑰ κ Boltzmann's constant, $0.6952 \text{ cm}^{-1} \text{ } ^\circ\text{K}^{-1}$
- ⑱ T_s Temperature of gas in light source, $^\circ\text{K}$
- ⑰ M_s, M_a Mass of molecules in light source and absorber, respectively, gm
- ⑱ c Velocity of light, $3 \times 10^{10} \text{ cm/sec}$
- ⑱ T_a Temperature of absorber gas, $^\circ\text{K}$

*Symbols are listed in the order of appearance in the text.

t	Transmissivity, fractional transmission through an absorbing medium
$\Delta\nu$	Wavenumber increment, cm^{-1}
e	Electronic charge, 4.80×10^{-10} esu
m	Electron mass, 9.11×10^{-28} gm
$N_{J''}$	Number density of molecules in the lower state, J'' , cm^{-3}
$f_{J'J''}$	Oscillator strength for the transition from the upper state J' to the lower state J''
N_0	Total number density of molecules, cm^{-3}
$J_{J''}$	Rotational quantum number for the lower state
S	Total electron spin quantum number
J_n	Electronic energy term value for the n^{th} electronic state (ground state, $n=0$), cm^{-1}
$G(v)$	Vibrational energy of the v^{th} vibrational state (ground state, $v=0$), cm^{-1}
$F(J'')$	Rotational energy of the J''^{th} rotational state, cm^{-1}
Q_e	Electronic partition function
Q_v	Vibrational partition function
Q_r	Rotational partition function
h	Planck's constant, 6.625×10^{-27} erg sec
B_v	Rotational constant for the v^{th} vibrational state (ground state, $v=0$), cm^{-1}
$f_{v'v''}$	Band oscillator strength for the $v' \leftrightarrow v''$ transition
$\nu_{J'J''}$	Wavenumber of the line corresponding to the transition $v'J' \rightarrow v''J''$, cm^{-1}
$\nu_{v'v''}$	Wavenumber at the bandhead of the (v', v'') band, cm^{-1}

30 S J''J'

Rotational strength, or Honl-London factor, for the $v'J' - v''J''$ vibrational - rotational transition

F_{u_j}

Rotational energy of the upper (u) electron state corresponding to the j^{th} spectral line, cm^{-1}

P

Radiant power falling on detector of spectrometer, radiant power units

$^\circ\lambda'$

Intensity distribution in image plane of spectrometer, intensity units

λ'

Instrument wavelength, cm

λ'_1, λ'_2

Instrument wavelength at limits of instrument wavelength interval at exit slit, cm

λ

Source wavelength, cm

$\Delta\lambda'_x$

Equivalent width of exit slit, cm

$\Delta\lambda'_e$

Equivalent width of entrance slit, cm

I_λ

Intensity distribution of source, intensity units

λ'_o

Instrument wavelength setting, cm

I_o

Intensity of continuum source, intensity units

I_{λ_o}

Intensity of monochromatic source, intensity units

λ_o

Wavelength at center of source line, cm

30 S J' a'

Spectral line j

I_a, I_b, I_c

Intensity of monochromatic lines used for illustration, intensity units

$\lambda'_a, \lambda'_b, \lambda'_c$

Instrument wavelength of lines used for illustration, cm

$\lambda_a, \lambda_b, \lambda_c$

Source wavelength of lines used for illustration, cm

$P_{\lambda'_o}$

Radiant power received by detector for the line at wavelength, λ'_o , radiant power units

11 w

12 Y

14 P

Pressure